AD-A164 166 THE AXIAL INJECTION TEM ORBITRON MASER(U) NAVAL RESEARCH LAB WASHINGTON DC J M BURKE ET AL. 31 JAN 86 NRL-MR-5675 1/1

UNCLASSIFIED F/G 20/5 NL

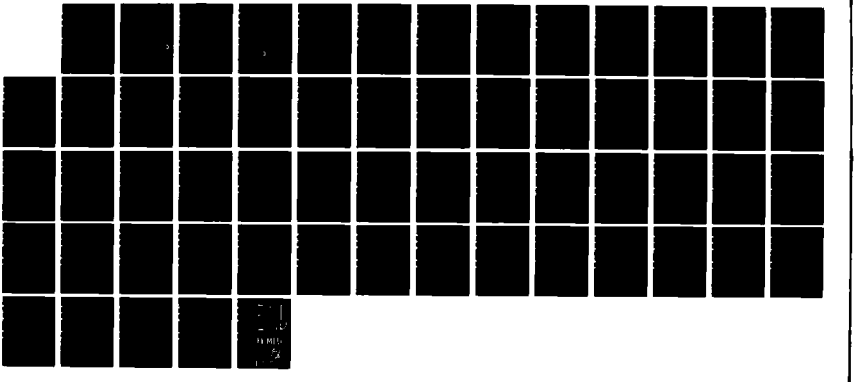

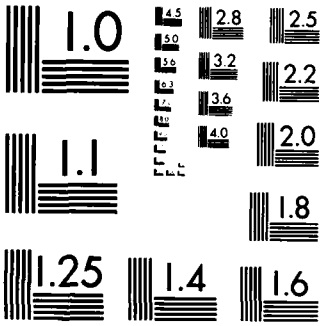

MICROCOPY RESOLUTION TEST CHART

)ARDS-1963-A

NRL Memorandum Report 5675

The Axial Injection TEM Orbitron Maser

JOHN M. BURKE AND WALLACE M. MANHEIMER

Plasma Physics Division

and

EDWARD OTT

Department of Electrical Engineering and
Department of Physics and Astronomy
University of Maryland
College Park, Maryland 20742

January 31, 1986

NAVAL RESEARCH LABORATORY
Washington, D.C.

SECURITY CLASSIFICATION OF THIS PAGE

REPORT DOCUMENTATION PAGE

1a. REPORT SECURITY CLASSIFICATION UNCLASSIFIED	1b. RESTRICTIVE MARKINGS
2a. SECURITY CLASSIFICATION AUTHORITY	3. DISTRIBUTION / AVAILABILITY OF REPORT Approved for public release; distribution is unlimited.
2b. DECLASSIFICATION / DOWNGRADING SCHEDULE	
4. PERFORMING ORGANIZATION REPORT NUMBER(S) NRL Memorandum Report 5675	5. MONITORING ORGANIZATION REPORT NUMBER(S)
6a. NAME OF PERFORMING ORGANIZATION Naval Research Laboratory 6b. OFFICE SYMBOL (*If applicable*) Code 4740	7a. NAME OF MONITORING ORGANIZATION
6c. ADDRESS (*City, State, and ZIP Code*) Washington, DC 20375-5000	7b. ADDRESS (*City, State, and ZIP Code*)
8a. NAME OF FUNDING / SPONSORING ORGANIZATION Office of Naval Research 8b. OFFICE SYMBOL (*If applicable*)	9. PROCUREMENT INSTRUMENT IDENTIFICATION NUMBER
8c. ADDRESS (*City, State, and ZIP Code*) Arlington, VA 22217	10. SOURCE OF FUNDING NUMBERS PROGRAM ELEMENT NO.: 61153N PROJECT NO.: 47-0866-0-6 TASK NO.: RR011-09-41 WORK UNIT ACCESSION NO.: DN880-061

11. TITLE (*Include Security Classification*)

The Axial Injection TEM Orbitron Maser

12. PERSONAL AUTHOR(S)

Burke, J.M., Manheimer, W.M., and Ott, E.*

13a. TYPE OF REPORT	13b. TIME COVERED	14. DATE OF REPORT (*Year, Month, Day*)	15. PAGE COUNT
Interim	FROM _____ TO _____	1986 January 31	59

16. SUPPLEMENTARY NOTATION

*Department of Electrical Engineering and Department of Physics and Astronomy, University of Maryland, College Park, Maryland 20742

17. COSATI CODES		
FIELD	GROUP	SUB-GROUP

18. SUBJECT TERMS (*Continue on reverse if necessary and identify by block number*)

TEM orbitron amplifier, linear theory, axially injected electrons, coaxial waveguide, oscillator configuration, axial injection scheme, ~~magnetic mode~~

19. ABSTRACT (*Continue on ~~reverse~~ if necessary and identify by block number*)

We have completed the linear theory of the TEM orbitron maser ~~which~~ models the interaction of axially injected electrons orbiting the positively charged center conductor of a coaxial waveguide with the TEM waveguide mode. The theory treats electrons with arbitrary values of angular momentum. ~~We will present~~ the threshold values of the cavity Q multiplied by the electron beam power required for self-oscillation in a finite length oscillator configuration as well as the spacial growth rate calculated for an infinite length TEM orbitron amplifier. ~~We have also developed~~ the basic design equations for the axial injection scheme.

20. DISTRIBUTION / AVAILABILITY OF ABSTRACT	21. ABSTRACT SECURITY CLASSIFICATION
☒ UNCLASSIFIED/UNLIMITED ☐ SAME AS RPT. ☐ DTIC USERS	UNCLASSIFIED
22a. NAME OF RESPONSIBLE INDIVIDUAL John M. Burke	22b. TELEPHONE (*Include Area Code*) (202) 767-2654 22c. OFFICE SYMBOL Code 4740

DD FORM 1473, 84 MAR 83 APR edition may be used until exhausted. All other editions are obsolete.

SECURITY CLASSIFICATION OF THIS PAGE

CONTENTS

THE AXIAL INJECTION TEM ORBITRON MASER

I. INTRODUCTION

The development of the electron cyclotron maser (ECM) has made possible the efficient generation of high power millimeter wavelength electromagnetic waves. One drawback of these devices with respect to size and cost, however, is that they require large magnetic fields. Thus there is current interest in developing a high efficiency millimeter wave source that does not require the use of a large magnetic field. In this paper we propose and analyze a device configuration which appears to hold great promise in fulfilling this goal. This proposed device is essentially a modification of the basic orbitron maser concept (Alexeff and Dyer, 1980 a). The orbitron maser employs coaxial cylindrical geometry with the center conductor held at a positive potential with respect to the outer conductor, as shown in Fig. 1. Electrons are radially confined by the positive potential of the center conductor and orbit around it.

In the earliest orbitron experiments, electrons were introduced into the cavity by creating a glow discharge between the center and outer conductor (Alexeff and Dyer, 1980 a,b). The electrons were axially confined by the fringing fields provided by conducting end caps held at the potential of the outer conductor. Broadband microwave emission was observed in a series of 25 ns bursts of radiation which occurred about 50 μs after the center conductor was pulsed to a high positive potential. Later experiments were able to achieve higher frequency operation by using an open cylindrical outer conductor and a center conductor with sharp periodic radial steps to provide an axial restoring force to confine the electrons (Alexeff and Dyer, 1983, 1984).

The theoretical explanation that was given to describe the operation of the orbitron experiments was that electrons executing circular orbits around the center conductor are negative mass unstable and would therefore exhibit a maser interaction (Alexeff and Dyer, 1980 a; Lau and Chernin, 1984 a,b; Alexeff, 1985). Using the notation of Fig. 1, the frequency of a nonrelativistic electron orbiting the center conductor in a circular orbit of radius r is

$$f = \frac{2.111}{r(mm)} \sqrt{\frac{V_0(kV)}{\ln\left(\frac{b}{a}\right)}} \text{ GHz} \qquad (1)$$

Manuscript approved November 21, 1985.

A voltage much larger than that used in the experiments is required for an electron in a circular orbit to interact with a TE mode because the azimuthal electric field component of any TE mode is large only at distances far from the center conductor. Indeed, the boundary condition on the electric fields in any coaxial waveguide is that the azimuthal electric field be zero at the conducting surfaces. Also, there is no interaction of the TEM cavity mode with an electron in a circular orbit. The assumption that electrons with circular orbits are even injected into the device seems unlikely. There is no mechanism for the electrons to gain a sufficient amount of angular momentum to achieve a circular orbit using the glow discharge radial electron injection scheme. Thus, if the emission process is indeed a maser interaction due to the negative mass nature of the electron's orbit, it is probable that it comes about through electrons with highly eccentric low angular momentum orbits interacting with TE or TEM waveguide modes at high harmonics of their radial oscillation frequency. An axial view of a low angular momentum electron orbit in an orbitron is shown in Fig. 2. Another difficulty complicating an understanding of the emission process of Alexeff and Dyer (1980a) and Alexeff (1985) is that there is no clear means for electrons to be removed from the cavity once they have transferred their energy to the radiation fields. Low energy electrons that are confined in the cavity may reabsorb energy from the radiation fields producing a relaxation oscillation. Indeed, it appears that it is some type of a relaxation oscillation that is observed experimentally (Alexeff and Dyer, 1980 b). Alternatively, it has been proposed that the microwave emission process in the glow discharge radial injection orbitron maser is due to the nonlinear wave-wave coupling of counterstreaming plasma waves (Schumacher and Harvey, 1984).

We will demonstrate that a high frequency, high efficiency orbitron maser that operates at high power levels can be realized by using an axial electron injection scheme. Electrons would be injected with a large value of axial momentum in a region with a low radial electric field. They would then be adiabatically compressed into the interaction region where the radial electric field is large. The adiabatic compression process has the advantage that it increases the electron density as well as the ratio of their perpendicular to parallel energy. The electrons would not be axially trapped in the interaction region as in the early orbitron experiments but would rapidly transit the interaction region where they would resonantly transfer their energy to the radiation fields. This injection scheme is very similar to the one used in most ECM devices which have been demonstrated to operate at high powers with high efficiencies (Hirshfield, 1979). The proposed axial injection orbitron maser would also operate in high vacuum, as is the case with most ECM devices. Most importantly, axial injection allows one to maximize the efficiency of the maser interaction by providing a means to produce an electron beam whose distribution function is optimized for the power level requirements of the device. It also provides a means to optimally position the electron beam to interact with a given waveguide or cavity mode.

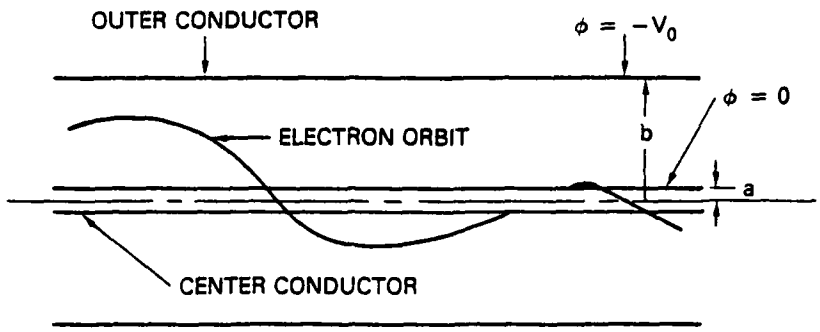

Figure 1. The orbitron configuration.

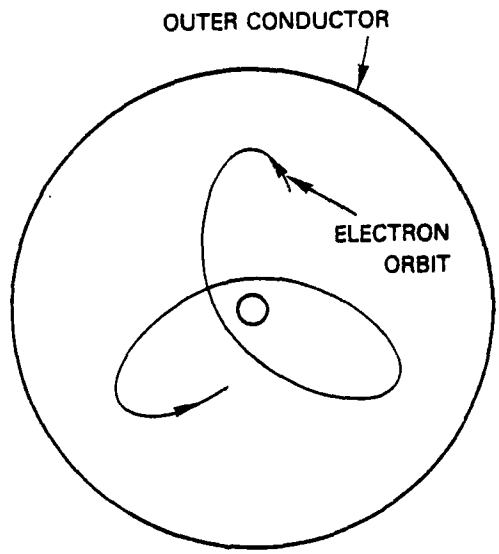

Figure 2. An axial view of an electron orbit.

Since for high harmonic operation we wish to take advantage of the structure of an electron orbit with a small minimum radius, the natural inclination is to examine modes with the largest fields near the center conductor. For this reason, we restrict our attention to TEM modes. In these, E_r and B_θ are both proportional to $1/r$ between the center and outer conductor. We have succeeded in analyzing the interaction of a TEM waveguide or cavity mode with low angular momentum electrons transiting the interaction region of an orbitron. This allows us to quantify the spacial growth rate for an infinite length traveling wave amplifier, as well as the threshold values of the cavity Q multiplied by the electron beam power required for self-oscillation in a finite length oscillator configuration. We have also developed the basic design equations necessary for the axial electron injection scheme.

The chapter is organized as follows. Section II presents the linear theory of the TEM orbitron maser. The dispersion relation for the axially uniform orbitron is derived by solving the linearized Vlasov equation by the method of characteristics. The integration over unperturbed orbits is performed by expressing the radial velocity of the electron multiplied by the radial part of the electric field's eigenfunction in a Fourier series. The radial part of the eigenfunction for the TEM mode has a particularly simple form, $1/r$. It will be shown that the interaction strength at a given harmonic of the radial oscillation frequency is proportional to the square of the Fourier coefficient for that frequency in the Fourier series expansion of the electron's radial velocity divided by its radius. The radial oscillation period for a nonrelativistic electron and other quantities having to do with the electron orbits in an orbitron which are necessary to evaluate the linear theory of the orbitron interaction are calculated in Section III. It will be shown that σ, which is defined as the ratio of the maximum to the minimum radius of the electron's orbit, is an important parameter. Specifically, the maximum harmonic number for which there can be a strong interaction is roughly $\sigma/2$. In Section IV we use the technique developed in Section II to calculate the power transferred from the electron beam to the radiation fields as the beam traverses a finite length cavity. The results of this calculation are combined with the definition of the cavity Q and an expression for the energy stored in the cavity in terms of the radiation electric field amplitude to find the beam power required to make the cavity self-oscillate. A cold beam distribution function in which each electron is assumed to have a single value of energy, angular momentum and axial momentum is presented in Section V. This distribution function allows the results of Sections II and IV, which are given in terms of a general distribution function, to be easily evaluated. Section VI presents the results for the infinite length traveling wave amplifier and the finite length oscillator configurations. The spacial growth rate is given versus frequency and beam parameters for the traveling wave amplifier. For the finite length oscillator, we plot the cavity Q multiplied by the threshold beam power required for self-oscillation versus the voltage between the center and outer conductor and beam parameters. Finally, in Section VII we discuss the consistency of the approximations used in the

theory, some mode selection schemes, and present a conceptual design of the beam injection system. We also use the constancy of the angular momentum of an electron in a TEM orbitron maser with an azimuthally symmetric electron beam to calculate the maximum possible efficiency of the device.

II. PHYSICAL MODEL: THE AXIALLY UNIFORM ORBITRON

The configuration of the orbitron maser that we will describe is shown in Figures 1 and 2. It consists of an electron beam propagating axially through a coaxial waveguide of circular cross section with inner radius a and outer radius b. The axis of the electron beam coincides with that of the waveguide. The electrons are radially confined by the electric field between the center and outer conductors of the waveguide, and move in axis encircling orbits with a substantial fraction of their kinetic energy transverse to the axis.

The following simplifying assumptions are made:

i) The electron beam distribution function and the cavity fields are both independent of the azimuthal angle θ.

ii) The electron beam is of low enough density so that its self-electrostatic field can be neglected compared to the static confining electric field due to the applied voltage difference between the inner and outer surfaces of the waveguide.

iii) The cavity fields are a first order perturbation of the static confining electric field.

iv) The perturbed distribution function f^1 is of first order with respect to the initial distribution function f^0.

The TEM mode is the lowest order mode for a coaxial waveguide and we shall restrict the analysis of the maser action in the orbitron to this mode. The TEM mode has a particularly simple structure which greatly simplifies the analysis compared with that of the TE mode which also should give rise to a maser interaction.

In this section, we examine the orbitron interaction by calculating the dispersion relation for an axially uniform system. This will set the stage for the calculations in Section IV of start oscillation conditions for a finite length cavity, as well as show how to handle the effect of the complex orbit.

If we use the convention shown in Figure 1 for the potentials on the conductors, the electrostatic potential energy of an electron is

$$q\phi(r) = P_0 \ln\left(\frac{r}{a}\right), \tag{2}$$

where

$$P_0 = \frac{eV_0}{ln\left[\frac{b}{a}\right]}. \tag{3}$$

The Hamiltonian can then be written

$$H = \frac{p_r^2}{2m} + \frac{P_\theta^2}{2mr^2} + \frac{p_z^2}{2m} + P_0\, ln\left[\frac{r}{a}\right], \tag{4}$$

where

$$\mathbf{p} = m\mathbf{v}, \tag{5}$$

and the electron is assumed to be nonrelativistic. Now, since the Hamiltonian is independent of time, θ and z we have three constants of the motion H, P_θ and p_z, where

$$P_\theta = r\, p_\theta = mr^2\, \dot{\theta}. \tag{6}$$

To find the motion of an electron we first determine the radius as a function of time by combining Equations (4) and (5),

$$dt = \frac{dr}{\sqrt{\frac{2H}{m} - \frac{P_\theta^2}{m^2r^2} - \frac{p_z^2}{m^2} - \frac{2P_0}{m}\, ln\left[\frac{r}{a}\right]}}. \tag{7}$$

Once $r(t)$ is known, θ as a function of time can be computed by integrating Equation (6) in time.

The angular momentum term in Equation (7) provides an outward radial force which dominates at small r, the electrostatic potential provides an inward force which dominates at large r. Thus the orbit has an inner and outer radial turning point, r_i and r_o. At each turning point, the radial velocity is, of course, zero.

The orbit is characterized by a shape, which is invariant given the constants of motion, and an initial value. For the more conventional case of a sinusoidal or circular orbit, the former corresponds to the amplitude and frequency, while the latter corresponds to the phase. To specify the shape of the orbit, we will consider an orbit such that $t = 0$ is the time at which $r = r_o$ and define this orbit as

$r = R(t)$ and $v_r = V(t)$. It is important to note that $R(t)$ is an even function of t while $V(t)$ is an odd function of t. Schematics of $R(t)$ and $V(t)$ are shown in Figure 3. The orbit has a full period $T(H, P_\theta, p_z)$ which depends only on the constants of the motion.

To calculate the dispersion relation for the orbitron interaction in an axially uniform system we use Maxwell's equations to find an equation that relates the perturbed electric field in the waveguide to the perturbed current. We then find the perturbed current in terms of the perturbed electric field by integrating Vlasov's equation over unperturbed orbits. Combining the two relations yields the dispersion relation.

Now, starting with Maxwell's equations

$$\nabla \cdot \mathbf{E} = \frac{\rho}{\epsilon_0}, \tag{8}$$

$$\nabla \cdot \mathbf{B} = 0, \tag{9}$$

$$\nabla \times \mathbf{E} + \frac{\partial \mathbf{B}}{\partial t} = 0, \tag{10}$$

$$\nabla \times \mathbf{B} - \frac{1}{c^2} \frac{\partial \mathbf{E}}{\partial t} = \mu_0 \mathbf{J}, \tag{11}$$

we combine Equations (10) and (11) with an assumed time dependence of $e^{-i\omega t}$ to get an equation for the electric field

$$\nabla \times \nabla \times \mathbf{E} - \frac{\omega^2}{c^2} \mathbf{E} = i\omega\mu_0 \mathbf{J}. \tag{12}$$

To proceed, we expand $\mathbf{E}$ as a linear superposition of orthogonal vacuum waveguide modes. In this paper we focus specifically on the TEM mode, because this mode has maximum electric field near the center conductor, where, as we will see, the orbit has the most harmonic structure. The waveguide fields of the TEM mode are given by

$$\mathbf{E}^1(r, \theta, z, t) = E_1 \frac{a}{r} e^{i(kz - \omega t)} \hat{r}, \tag{13}$$

$$\mathbf{B}^1(r, \theta, z, t) = E_1 \frac{a}{cr} e^{i(kz - \omega t)} \hat{\theta}, \tag{14}$$

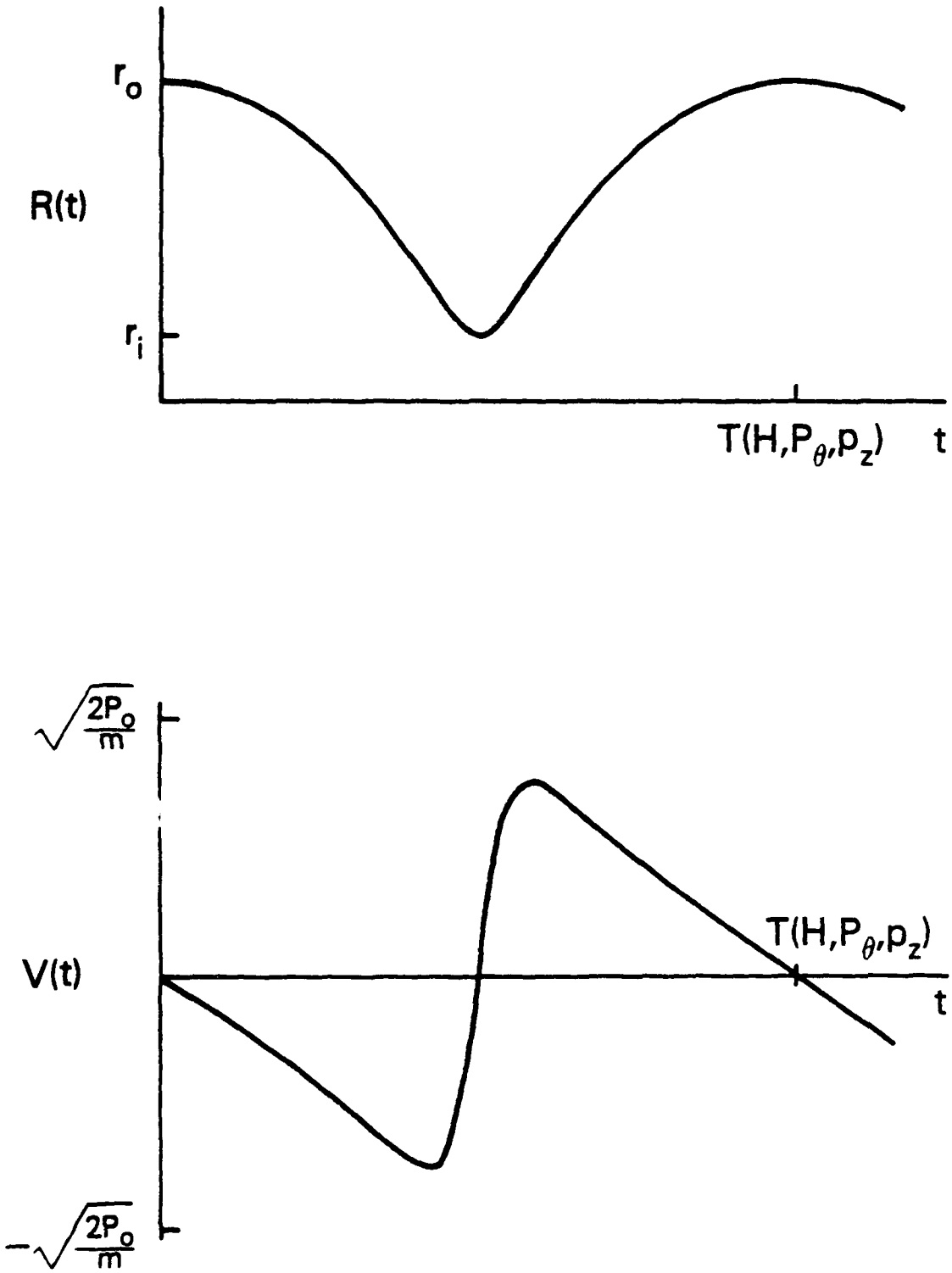

Figure 3. The radius and radial velocity of an electron orbiting the center conductor versus time.

and we assume that the beam current is small so that the mode is nearly a vacuum mode. This is analogous to assumptions made in calculating the linear theory of the ECM. Then, as discussed by Ott and Manheimer (1975), once we determine the form of $J_r^1(r, \theta, z, t)$ driven by the waveguide fields given by Equations (13) and (14), we take the dot product of Equation (12) with the complex conjugate of Equation (13) and integrate over the waveguide cross section to find the dispersion relation,

$$\left[k^2 - \frac{\omega^2}{c^2}\right] \int |\mathbf{E}^1|^2 \, r dr d\theta = i\omega\mu_0 \int \mathbf{E}^{1*} \cdot \mathbf{J}^1 \, r dr d\theta \,. \tag{15}$$

Finding the perturbed current means integrating over the unperturbed orbits which are unspecified as yet, and quite complicated. However, the effect of this complex orbit can be characterized by a single parameter as we will see shortly.

The perturbed current density, in terms of the perturbed distribution function, is given by

$$J_r^1(r, \theta, z, t) = -e \int \mathrm{v}_r \, f^1 \, (\mathbf{r}, \mathbf{p}, t) \, d^3p \,. \tag{16}$$

We use the Vlasov equation,

$$\frac{\partial f(\mathbf{r}, \mathbf{p}, t)}{\partial t} + \mathbf{v} \cdot \frac{\partial f(\mathbf{r}, \mathbf{p}, t)}{\partial \mathbf{r}} + q(\mathbf{E}\,(\mathbf{r}, t) + \mathbf{v} \times \mathbf{B}\,(\mathbf{r}, t)) \cdot \frac{\partial f(\mathbf{r}, \mathbf{p}, t)}{\partial \mathbf{p}} = 0 \,, \tag{17}$$

to find the perturbed distribution function, where

$$f(\mathbf{r}, \mathbf{p}, t) = f^0(\mathbf{r}, \mathbf{p}) + f^1(\mathbf{r}, \mathbf{p}, t) \,. \tag{18}$$

Then, to first order

$$f^1(\mathbf{r}, \mathbf{p}, t) = e \int_{-\infty}^{t} dt' \left[\mathbf{E}^1(\mathbf{r}', t') + \mathbf{v}\,'(\mathbf{r}', t') \times \mathbf{B}^1(\mathbf{r}', t') \right] \frac{\partial f^0(\mathbf{r}', \mathbf{p}')}{\partial \mathbf{p}'} \,. \tag{19}$$

The quantities r and v_r implicit in Equation (19) are evaluated along the unperturbed orbit, where the orbit is initialized by specifying that the velocity $V(t)$ is v_r and the position $R(t)$ is r at time $t = t'$. If $\hat{t}(r, \mathrm{v}_r)$ is the time between 0 and $T(H, P_\theta, p_z)$ such that $V(\hat{t}) = \mathrm{v}_r$ and $R(\hat{t}) = r$, the unperturbed orbit is specified by $R(y)$ and $V(y)$ where

$$y = t' - t + \hat{t}(r, \mathrm{v}_r) \,. \tag{20}$$

Inserting Equations (13) and (14) into Equation (19) and using the fact that

$$\frac{\partial f^0(H, P_\theta, p_z)}{\partial p_r} = \mathrm{v}_r \frac{\partial f^0(H, P_\theta, p_z)}{\partial H} \,, \tag{21}$$

we find an expression for the perturbed distribution function,

$$f^1(\mathbf{r}, \mathbf{p}, t) = e\ a\ E_1 \left[\left(1 - \frac{v_z}{c} \right) \frac{\partial f^0}{\partial H} + \frac{1}{c} \frac{\partial f^0}{\partial p_z} \right] \int_{-\infty}^{t} dt'\, e^{i(kz'(t') - \omega t)} \frac{V(t' - t + \hat{t}(r, v_r))}{R(t' - t + \hat{t}(r, v_r))}. \quad (22)$$

Since $V(y)/R(y)$ is an odd function of y, it can be expanded as a sine series

$$\frac{V(y)}{R(y)} = \sum_{s=1}^{\infty} a_s(H, P_\theta, p_z) \sin\left(s\Omega(H, P_\theta, p_z)\, y\right), \quad (23)$$

where $\Omega(H, P_\theta, p_z) = 2\pi/T(H, P_\theta, p_z)$ and $a_s(H, P_\theta, p_z)$ is the Fourier coefficient, which is a function of the constants of the motion.

Now, if we let

$$x = t' - t, \quad (24)$$

$$v_z' = v_z, \quad (25)$$

then

$$kz'(t') = kz + kv_z x, \quad (26)$$

$$t' = x + t. \quad (27)$$

Inserting Equations (23), (26) and (27) into Equation (22) yields the perturbed distribution function,

$$f^1(\mathbf{r}, \mathbf{p}, t) = e\ a\ E_1 \left[\left(1 - \frac{v_z}{c} \right) \frac{\partial f^0}{\partial H} + \frac{1}{c} \frac{\partial f^0}{\partial p_z} \right]$$

$$\sum_{s=1}^{\infty} a_s(H, P_\theta, p_z) \int_{-\infty}^{0} dx\ e^{i(kz - \omega t + (kv_z - \omega)x)} \sin\left(s\Omega(H, P_\theta, p_z)(x + \hat{t}(r, v_r))\right)$$

$$= -\frac{e\ a\ E_1}{2} \left[\left(1 - \frac{v_z}{c} \right) \frac{\partial f^0}{\partial H} + \frac{1}{c} \frac{\partial f^0}{\partial p_z} \right] \quad (28)$$

$$\sum_{s=1}^{\infty} a_s(H, P_\theta, p_z) \left\{ \frac{e^{i(kz - \omega t + s\Omega(H, P_\theta, p_z)\hat{t}(r, v_r))}}{(s\Omega(H, P_\theta, p_z) - \omega + kv_z)} + \frac{e^{i(kz - \omega t - s\Omega(H, P_\theta, p_z)\hat{t}(r, v_r))}}{(s\Omega(H, P_\theta, p_z) + \omega - kv_z} \right\},$$

and combining Equations (16) and (28) we find that

$$i\omega\mu_0 J_r = i\mu_0\,\omega\,\frac{e^2 a\,E_1}{2}\sum_{s=1}^{\infty}\int d^3p\; a_s(H,\,P_\theta,\,p_z)\;v_r$$

$$\left[\left(1-\frac{v_z}{c}\right)\frac{\partial f^0}{\partial H}+\frac{1}{c}\,\frac{\partial f^0}{\partial p_z}\right]\left\{\frac{e^{i(kz-\omega t+s\Omega(H,\,P_\theta,\,p_z)\hat{t}(r,\,v_r))}}{(s\Omega(H,\,P_\theta,\,p_z)-\omega+kv_z)}+\frac{e^{i(kz-\omega t-s\Omega(H,\,P_\theta,\,p_z)\hat{t}(r,\,v_r))}}{(s\Omega(H,\,P_\theta,\,p_z)+\omega-kv_z)}\right\}. \tag{29}$$

Equations (13), (15) and (29) then yield the dispersion relation

$$\left(k^2-\frac{\omega^2}{c^2}\right)a^2\,ln\left(\frac{b}{a}\right)=i\mu_0\omega\,\frac{e^2a^2}{2}$$

$$\sum_{s=1}^{\infty}\int dr\int d^3p\;v_r\;a_s\;(H,\,P_\theta,\,p_z)\left[\left(1-\frac{v_z}{c}\right)\frac{\partial f^0}{\partial H}+\frac{1}{c}\,\frac{\partial f^0}{\partial p_z}\right] \tag{30}$$

$$\left\{\frac{e^{i(s\Omega(H,\,P_\theta,\,p_z)\hat{t}(r,\,v_r))}}{(s\Omega(H,\,P_\theta,\,p_z)-\omega+kv_z)}+\frac{e^{-i(s\Omega(H,\,P_\theta,\,p_z)\hat{t}(r,\,v_r))}}{(s\Omega(H,\,P_\theta,\,p_z)+\omega-kv_z)}\right\}.$$

Notice that at this point there is still a fairly complex dependence on r and v_r through the exponential of $\Omega(H,\,P_\theta,\,p_z)\hat{t}(r,\,v_r)$. Utilizing the Jacobian to transform the integration over d^3p to an integration over $dHdP_\theta dp_z$,

$$\left(k^2-\frac{\omega^2}{c^2}\right)ln\left(\frac{b}{a}\right)=i\mu_0\,\omega\,\frac{e^2}{2}\sum_{s=1}^{\infty}\int_a^b dr\int dH\;dP_\theta dp_z\;\frac{1}{r}\,\frac{v_r}{|v_r|}\sum_{\pm}$$

$$a_s(H,\,P_\theta,\,p_z)\left[\left(1-\frac{v_z}{c}\right)\frac{\partial f^0}{\partial H}+\frac{1}{c}\,\frac{\partial f^0}{\partial p_z}\right] \tag{31}$$

$$\left\{\frac{e^{i(s\Omega(H,\,P_\theta,\,p_z)\hat{t}_\pm(r,\,v_r))}}{(s\Omega(H,\,P_\theta,\,p_z)-\omega+kv_z)}+\frac{e^{-i(s\Omega(H,\,P_\theta,\,p_z)\hat{t}_\pm(r,\,v_r))}}{(s\Omega(H,\,P_\theta,\,p_z)+\omega-kv_z)}\right\},$$

where the summation over $\pm$ is a summation over $\hat{t}_+(r,\,v_r)$ and $\hat{t}_-(r,\,v_r)$. Here $\hat{t}_+(r,\,v_r)$ is the time for the particle to reach r with positive v_r. Using the time origin of Figure 3, we see that $\frac{T}{2}(H,\,P_\theta,\,p_z)<\hat{t}_+(r,\,v_r)<T(H,\,P_\theta,\,p_z)$. Similarly, $\hat{t}_-(r,\,v_r)$ is the time required for the particle to

reach r with negative radial velocity and $0 < \hat{t}_-(r, v_r) < \frac{T}{2}(H, P_\theta, p_z)$. We now bring the integration over radius inside the integration over momentum space and perform the integration over radius by changing the variable of integration to $\hat{t}(r, v_r)$. Then

$$\frac{dr}{r} = \frac{V(\hat{t})}{R(\hat{t})}\, d\hat{t}, \tag{32}$$

and Equation (31) becomes

$$\left[k^2 - \frac{\omega^2}{c^2}\right] ln\left[\frac{b}{a}\right] = i\mu_0\,\omega\,\frac{e^2}{2}\sum_{s=1}^{\infty}\int dHdP_\theta dp_z\; a_s(H, P_\theta, p_z)\left[\left[1 - \frac{v_z}{c}\right]\frac{\partial f^0}{\partial H} + \frac{1}{c}\frac{\partial f^0}{\partial p_z}\right]$$

$$\left\{\int_{\frac{T}{2}(H, P_\theta, p_z)}^{T(H, P_\theta, p_z)} \frac{V(\hat{t})}{R(\hat{t})}\, d\hat{t}\left[\frac{e^{i(s\Omega(H, P_\theta, p_z)\hat{t})}}{(s\Omega(H, P_\theta, P_z) - \omega + kv_z)} + \frac{e^{-i(s\Omega(H, P_\theta, p_z)\hat{t})}}{(s\Omega(H, P_\theta, p_z) + \omega - kv_z)}\right]\right. \tag{33}$$

$$\left. - \int_{\frac{T}{2}(H, P_\theta, p_z)}^{0} \frac{V(\hat{t})}{R(\hat{t})}\, d\hat{t}\left[\frac{e^{i(s\Omega(H, P_\theta, p_z)\hat{t})}}{(s\Omega(H, P_\theta, p_z) - \omega + kv_z)} + \frac{e^{-i(s\Omega(H, P_\theta, p_z)\hat{t})}}{(s\Omega(H, P_\theta, p_z) + \omega - kv_z)}\right]\right\}.$$

Now, we have

$$\frac{V(\hat{t})}{R(\hat{t})} = \sum_{s=1}^{\infty} a_s(H, P_\theta, p_z)\sin(s\Omega(H, P_\theta, p_z)\hat{t}). \tag{34}$$

Inserting Equation (34) into Equation (33) and integrating over $\hat{t}$ we obtain the dispersion relation for a forward traveling wave in an axially uniform orbitron in its final form

$$\left[k^2 - \frac{\omega^2}{c^2}\right] ln\left[\frac{b}{a}\right] = -\frac{\mu_0 e^2 \omega}{4}\sum_{s=1}^{\infty}\int dHdP_\theta dp_z \left\{\left[\left[1 - \frac{v_z}{c}\right]\frac{\partial f^0}{\partial H} + \frac{1}{c}\frac{\partial f^0}{\partial p_z}\right]\right.$$

$$\left. T(H, P_\theta, p_z)\, a_s^2(H, P_\theta, p_z)\left[\frac{1}{(s\Omega(H, P_\theta, p_z) - \omega + kv_z)} - \frac{1}{(s\Omega(H, P_\theta, p_z) + \omega - kv_z)}\right]\right\}. \tag{35}$$

Equation (35) is written in terms of a general unperturbed distribution function $f^0(H, P_\theta, p_z)$. We will present a specific distribution function in Section V which allows us to calculate, in Section VI, the spacial growth rate of the forward traveling wave as a function of frequency and the electron beam parameters.

III. ELECTRON ORBITS

We are interested in the details of the radial motion of an electron confined in the logarithmic potential well provided by the configuration shown in Figures 1 and 2. To calculate the radial oscillation period of the orbit, $T(H, P_\theta, p_z)$, in terms of the constants of the motion, we take Equation (7) and integrate from r_i to r_o

$$\frac{T}{2}(H, P_\theta, p_z) = \sqrt{\frac{m}{2}} \int_{r_i}^{r_o} \frac{dr}{\sqrt{H - \frac{P_\theta^2}{2mr^2} - \frac{p_z^2}{2m} - P_0 \ln\left[\frac{r}{a}\right]}}, \tag{36}$$

where r_0 and r_i are the roots of the equation

$$v_r = \sqrt{\frac{2}{m}} \sqrt{H - \frac{P_\theta^2}{2mr^2} - \frac{p_z^2}{2m} - P_0 \ln\left[\frac{r}{a}\right]} = 0. \tag{37}$$

To put Equation (36) into a simpler form we transform variables as follows. Let

$$r = \frac{P_\theta}{\sqrt{2mP_0}} \frac{1}{\xi}, \tag{38}$$

and

$$\beta(H, P_\theta, p_z) = \frac{H}{P_0} - \frac{p_z^2}{2mP_0} - \ln\left[\frac{P_\theta}{\sqrt{2mP_0}a}\right]. \tag{39}$$

Equation (36) can then be written

$$T(H, P_\theta, p_z) = \frac{P_\theta}{P_0} \psi(\beta), \tag{40}$$

where

$$\psi(\beta) = \int_{\xi_o}^{\xi_i} \frac{d\xi}{\xi^2 \sqrt{\beta + \ln \xi - \xi^2}}, \tag{41}$$

and ξ_o and ξ_i are the two roots of the equation

$$\beta(H, P_\theta, p_z) + \ln(\xi) - \xi^2 = 0. \tag{42}$$

We can use the particularly simple form of Equation (40) to compute the derivatives $\frac{\partial T}{\partial H}$ and $\frac{\partial T}{\partial p_z}$ which are necessary to evaluate the general result given in Equation (35) for the specific distribution function that will be described in Section V. Indeed,

$$\frac{1}{T}\frac{\partial T(H, P_\theta, p_z)}{\partial H} = \frac{1}{P_0}\frac{d}{d\beta}\ln(\psi(\beta))$$

$$= \frac{1}{P_0}\chi(\beta) \tag{43}$$

and similarly

$$\frac{1}{cT}\frac{\partial T(H, p_\theta, p_z)}{\partial p_z} = -\frac{v_z}{c}\frac{1}{P_0}\chi(\beta)\,. \tag{44}$$

Now, when we evaluate the theory given in Section II, we choose to specify the constants of the motion P_θ and p_z in terms of the more physically interpretable parameters σ and α where σ is the ratio of the maximum to the minimum radius of the electron's orbit and α is the square root of the ratio of the electron's perpendicular energy to the parallel energy, that is

$$\sigma = \frac{r_o}{r_i} = \frac{\xi_i}{\xi_o}, \tag{45}$$

and

$$\alpha = \sqrt{\frac{H_\perp}{H_{||}}}. \tag{46}$$

We will now show that $\beta(H, P_\theta, p_z)$ is uniquely specified by the single quantity σ. Equating the left hand side of Equation (42) for the root ξ_i to the left hand side of Equation (42) for the root ξ_o and using Equation (45) we find the relation

$$\xi_o^2 = \frac{\ln(\sigma)}{\sigma^2 - 1}\,. \tag{47}$$

Inserting Equation (47) into Equation (42) then yields an equation for $\beta(H, P_\theta, p_z)$ in terms of σ

$$\beta(\sigma) = \frac{\ln(\sigma)}{\sigma^2 - 1} - \frac{1}{2}\ln\left[\frac{\ln(\sigma)}{\sigma^2 - 1}\right]. \tag{48}$$

The parameter $\chi(\beta)$ is therefore completely determined by the parameter σ and we define the function $\eta(\sigma)$ in terms of $\chi(\beta)$

$$\eta(\sigma) = \chi(\beta(\sigma)) . \tag{49}$$

A graph of $\eta(\sigma)$ versus σ is shown in Figure 4.

The radial oscillation period in terms of H, σ, and α is given by

$$T = a \sqrt{\frac{2m}{P_0}} \exp\left[\frac{\alpha^2 H}{(1+\alpha^2)P_0} - \frac{ln(\sigma)}{\sigma^2 - 1} \right] \zeta(\sigma) , \tag{50}$$

where

$$\zeta(x) = \int_1^x \frac{d\xi}{\xi^2 \sqrt{\frac{ln(\sigma)}{\sigma^2 - 1}(1 - \xi^2) + ln(\xi)}} . \tag{51}$$

The function

$$t\left(\frac{r_0}{r}\right) = a \sqrt{\frac{m}{2P_0}} \exp\left[\frac{\alpha^2 H}{(1+\alpha^2)P_0} - \frac{ln(\sigma)}{\sigma^2 - 1} \right] \zeta\left(\frac{r_0}{r}\right) \tag{52}$$

is the time it takes the electron to go from r_0 to r. To compute the radial oscillation period in the two limiting cases of a nearly circular orbit, $\sigma \to 1$, and in the zero angular momentum case where $\sigma \to \infty$ we note that

$$\zeta(1) = \pi \tag{53}$$

and

$$\zeta(\infty) = \sqrt{\pi} . \tag{54}$$

The function $\hat{T}(\sigma)$, where

$$\hat{T}(\sigma) = \frac{T}{a \sqrt{\frac{2m}{P_0}} \exp\left[\frac{\alpha^2 H}{(\alpha^2 + 1)P_0} \right]} , \tag{55}$$

is displayed in Figure 5.

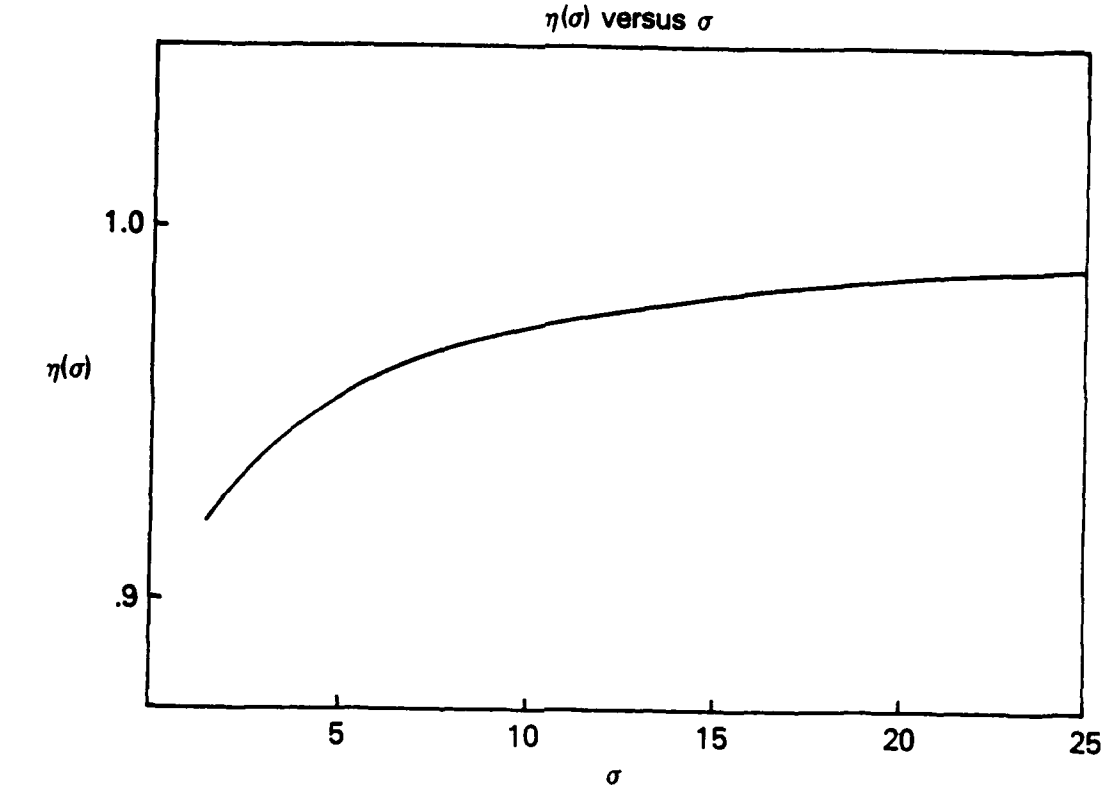

Figure 4. The parameter $\eta(\sigma)$ versus σ.

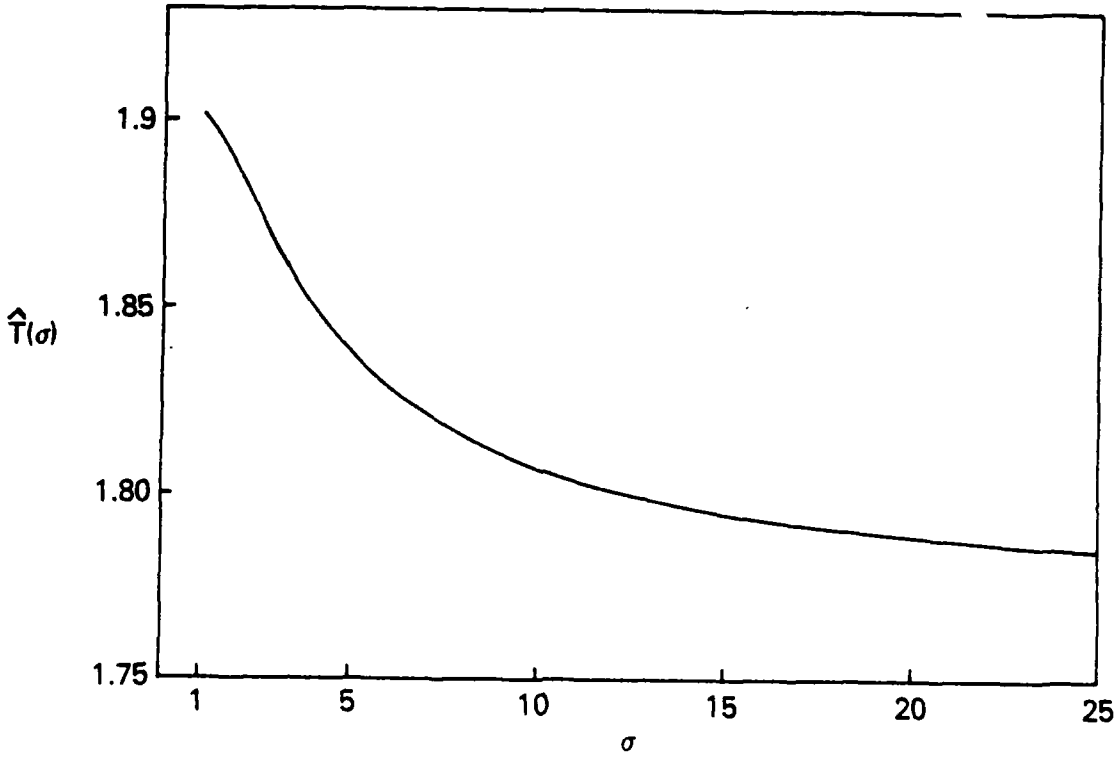

Figure 5. The normalized radial oscillation period versus σ.

To evaluate the expression given in Equation (35) for the dispersion relation for a forward traveling wave amplifier and the result of the oscillator calculation in the section that follows, we must also calculate the coefficient $a_s(H, P_\theta, p_z)$ in the Fourier series for $\frac{V(t)}{R(t)}$ given in Equation (23) and its derivatives with respect to H and p_z. That is

$$\frac{V(t)}{R(t)} = \sum_{s=1}^{\infty} a_s(H, P_\theta, p_z) \sin\left[\frac{2\pi s}{T(H, P_\theta, p_z)} t\right], \tag{56}$$

and therefore

$$a_s(H, P_\theta, p_z) = \frac{4}{T(H, P_\theta, p_z)} \int_0^{\frac{T}{2}(H, P_\theta, p_z)} \frac{V(t)}{R(t)} \sin\left[\frac{2\pi s}{T(H, P_\theta, p_z)} t\right] dt. \tag{57}$$

Now, if we define

$$\kappa_s \equiv \frac{T(H, P_\theta, p_z)}{2\pi} a_s(H, P_\theta, p_z), \tag{58}$$

and change variables to $r_0/r(t)$, we find that

$$\kappa_s = -\frac{2}{\pi} \int_1^{\sigma} \frac{dx}{x} \sin\left[s\pi \frac{\zeta(x)}{\zeta(\sigma)}\right]. \tag{59}$$

We see that κ_s is a function of only σ and $\kappa_s^2(\sigma)$ is plotted versus s/σ for various values of σ and s in Figure 6. To compute the value of s where $\kappa_s(\sigma)$ begins to decrease in amplitude, we combine Equations (57) and (58) and integrate by parts, to obtain

$$\kappa_s(\sigma) = \frac{4s}{T} \int_0^{\frac{T}{2}} \ln\left[\frac{r_o}{r(t)}\right] \cos(s\Omega t)\, dt. \tag{60}$$

The harmonic content of the radial oscillation period is principally determined by the motion of the electron near the minimum radius turning point, so we expand the $ln\left[\frac{r_o}{r(t)}\right]$ term in the integrand around $r(t) = r_i$ and examine its form. Using Equation (52), we find

$$ln\left[\frac{r_o}{r(t)}\right] = ln(\sigma)\left[1 - \frac{\zeta^2(\sigma)\sigma^2}{ln(\sigma)T^2}\left\{\frac{2\sigma^2 ln(\sigma)}{\sigma^2 - 1} - 1\right\}\left\{t - \frac{T}{2}\right\}^2 + \cdots\right] \tag{61}$$

$$\cong ln(\sigma) \cos(\tilde{\omega}(t - \frac{T}{2}))$$

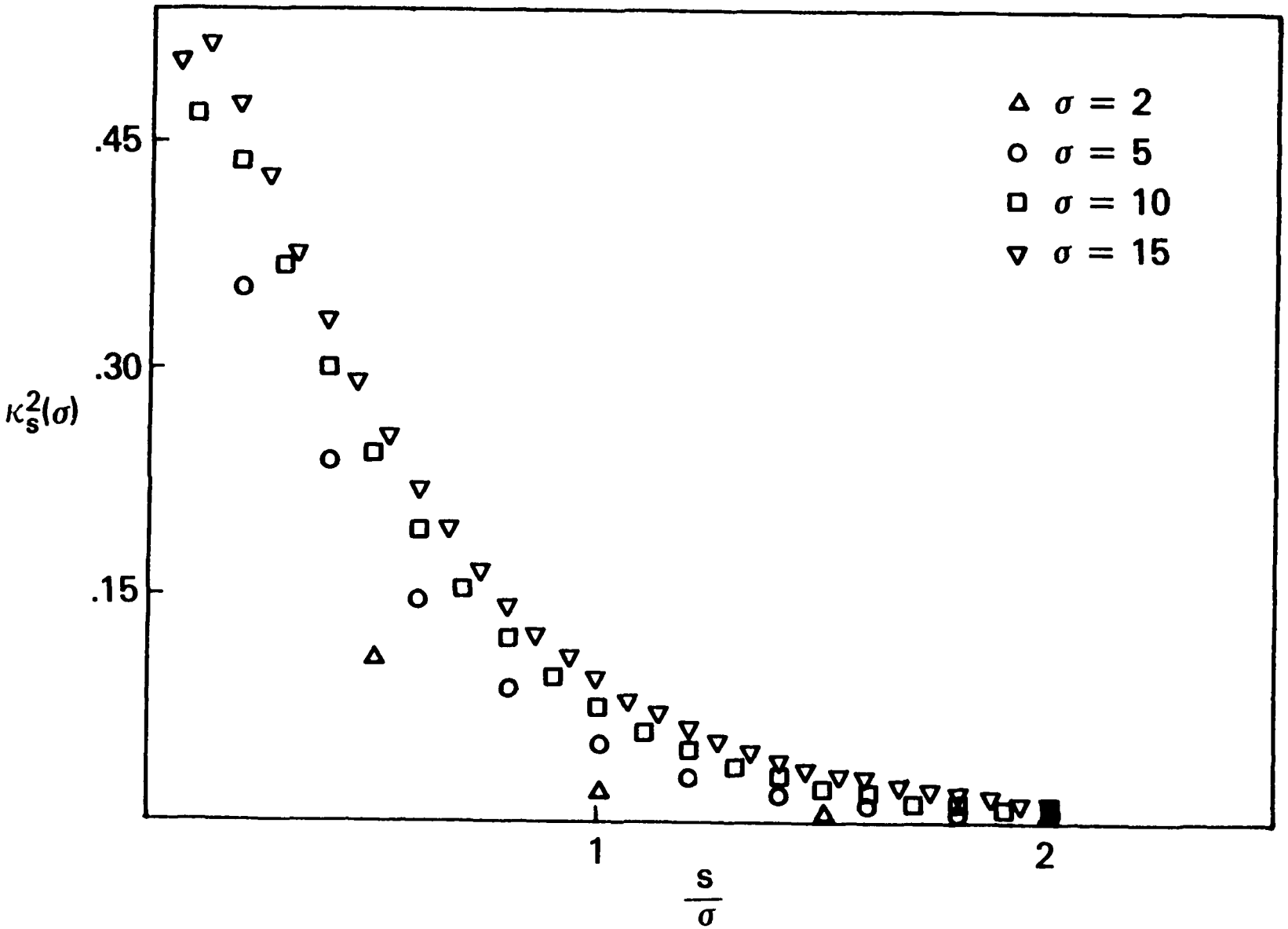

Figure 6. The coupling coefficient $\kappa_s^2(\sigma)$ versus harmonic number for various values of σ.

for $t \cong \frac{T}{2}$, where

$$\tilde{\omega} = \frac{\sigma\, \zeta(\sigma)\, \Omega}{\pi \sqrt{2 ln(\sigma)}} \sqrt{\frac{2\sigma^2 ln(\sigma)}{\sigma^2 - 1} - 1}\,. \tag{62}$$

The radial oscillation contains frequencies up to $\sim\tilde{\omega}$ and therefore $\kappa_s(\sigma)$ should begin to decrease in amplitude for

$$s\Omega > \tilde{\omega}\,, \tag{63}$$

or

$$\frac{s}{\sigma} \gtrsim \frac{\zeta(\sigma)}{\pi \sqrt{2 ln(\sigma)}} \sqrt{\frac{2\sigma^2 ln(\sigma)}{\sigma^2 - 1} - 1}\,. \tag{64}$$

Evaluating the expression on the right hand side of Equation (64), we find that $\kappa_s(\sigma)$ decreases for

$$\frac{s}{\sigma} \sim \frac{1}{2} \tag{65}$$

more or less independent of σ, as can be seen from Figure 6.

Last, to compute

$$\frac{\partial}{\partial H}\, a_s^2(H, P_\theta, p_z) \qquad \text{and} \qquad \frac{1}{c}\, \frac{\partial}{\partial p_z}\, a^2(H, P_\theta, p_z)\,,$$

we have

$$a_s(H, P_\theta, p_z) = \frac{2\pi}{T(H, P_\theta, p_z)}\, \kappa_s(\sigma)\,, \tag{66}$$

so

$$\frac{\partial}{\partial H}\, a_s^2(H, P_\theta, p_z) = 2\, a_s(H, P_\theta, p_z)\, 2\pi\, \frac{\partial}{\partial H}\, T^{-1}(H, P_\theta, p_z)\, \kappa_s(\sigma)$$

$$+ 2\, a_s(H, P_\theta, p_z)\, \frac{2\pi}{T(H, P_\theta, p_z)}\, \frac{\partial\, \kappa_s(\sigma)}{\partial H} \tag{67}$$

$$= -2\, \Omega^2\, \kappa_s^2(\sigma)\, \frac{1}{P_0} \left[\, \eta(\sigma) - \kappa_s'(\sigma)\, \right],$$

where

$$\kappa_s'(\sigma) = \frac{\dfrac{\partial \kappa_s(\sigma)}{\partial \sigma}}{\kappa_s(\sigma)} \frac{\partial \sigma}{\partial \beta} . \tag{68}$$

Similarly,

$$\frac{1}{c} \frac{\partial}{\partial p_z} a_s^2(H, P_\theta, p_z) = 2 \Omega^2 \kappa_s^2(\sigma) \frac{v_z}{c} \frac{1}{P_0} \left[\eta(\sigma) - \kappa_s'(\sigma) \right] . \tag{69}$$

IV. FINITE LENGTH CAVITY

We will now calculate the power transferred from an electron beam injected axially through the cavity that is shown schematically in Figure 7 to the fields of a TEM cavity mode. The assumptions (i) - (iv) used in Section II will again be applied here. The result of the transferred power calculation will then be used in Section VI to compute the threshold beam power required to make the cavity self-oscillate.

The cavity fields for a TEM mode in the cavity of Figure 7 are given by

$$\mathbf{E}^1(r, \theta, z, t) = E_1 \frac{a}{r} \sin(kz) \sin(\omega t) \hat{r} , \tag{70}$$

and

$$\mathbf{B}^1(r, \theta, z, t) = E_1 \frac{a}{cr} \cos(kz) \cos(\omega t) \hat{\theta} , \tag{71}$$

where

$$k = \frac{l\pi}{L} , \tag{72}$$

and

$$\omega = ck = l \frac{c\pi}{L} . \tag{73}$$

Using Equations (17), (18), (70) and (71) to find the perturbed distribution function by integrating over unperturbed orbits we find that

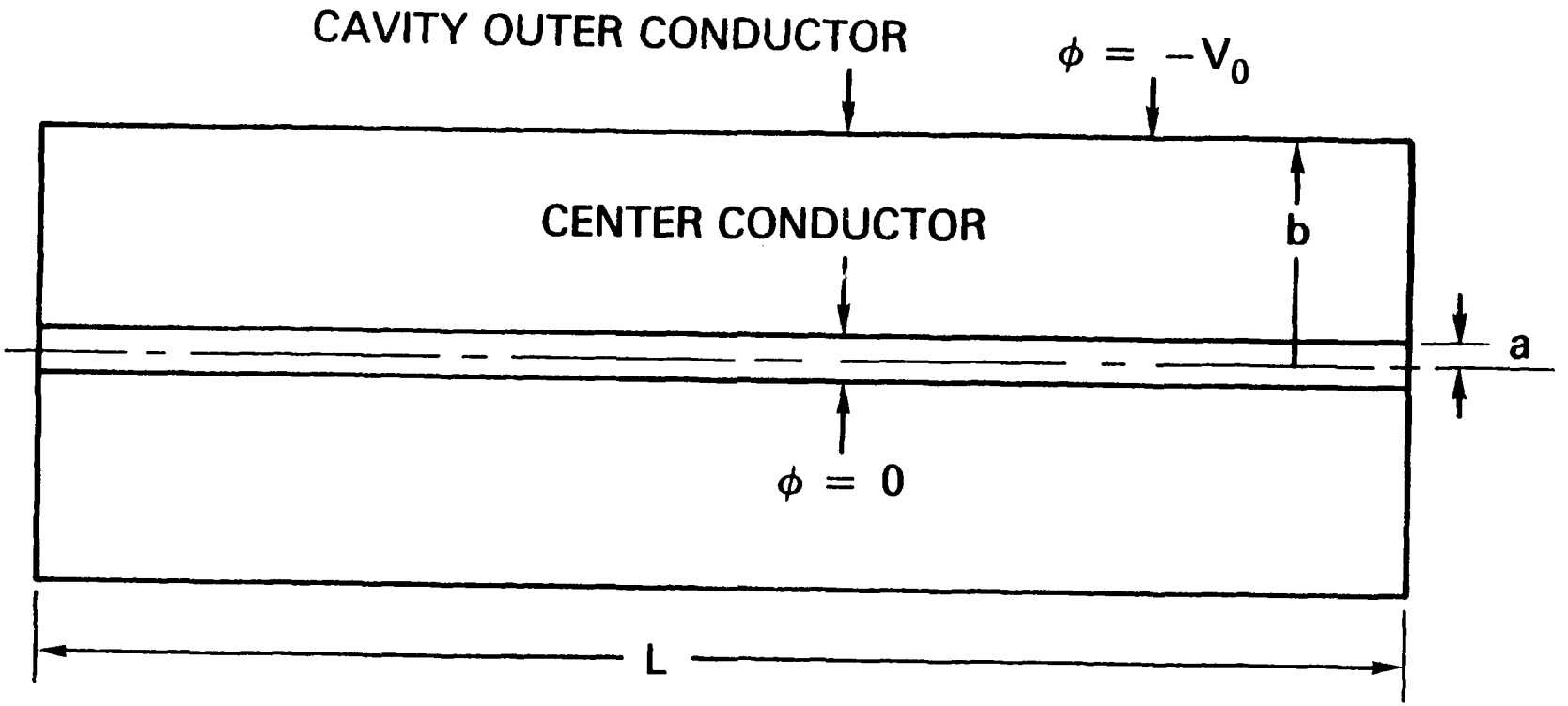

Figure 7. An idealized orbitron cavity.

$$f^1(\mathbf{r},\,\mathbf{p},\,t) = eaE_1 \int_{t-z/v_z}^{t} dt' \left[\sin\,(kz'(t'))\,\sin\,(\omega t')\,\frac{1}{r'(t')}\,\frac{\partial f^0}{\partial p_r'} \right.$$

$$\left. - \frac{v_z}{c}\cos\,(kz'(t'))\,\cos\,(\omega t')\,\frac{1}{r'(t')}\,\frac{\partial f^0}{\partial p_r'} + \frac{1}{c}\cos\,(kz'(t'))\,\cos(\omega t')\,\frac{v_r'(t')}{r'(t')}\,\frac{\partial f^0}{\partial p_z'} \right]. \qquad (74)$$

The integration is taken from the time the electron enters the cavity to time t. Proceeding in the same manner as we did between Equations (19) and (28) of Section II, we find the perturbed distribution function,

$$f^1(\mathbf{r},\,\mathbf{p},\,t) = \frac{eaE_1}{4}\sum_{s=1}^{\infty}\left\{ \frac{\partial f^0}{\partial H}\,a_s(H,\,P_\theta,\,p_z)\,(L_s(\omega,\,k) - L_s(\omega,\,-k) - L_s(-\omega,\,k) + L_s(-\omega,\,-k)) \right.$$

$$\left. + \left[\frac{1}{c}\,\frac{\partial f^0}{\partial p_z} - \frac{v_z}{c}\,\frac{\partial f^0}{\partial H} \right] a_s(H,\,P_\theta,\,p_z)\,(L_s(\omega,\,k) + L_s(\omega,\,-k) + L_s(-\omega,\,k) + L_s(-\omega,\,-k)) \right\}, \qquad (75)$$

where

$$L_s(\omega,k)$$

$$= \frac{\cos(s\Omega\,(H,P_\theta,p_z)\hat{t}(r,v_r) - \omega t - (s\Omega\,(H,P_\theta,p_z) - \omega)z/v_z) - \cos(s\Omega\,(H,P_\theta,p_z)\hat{t}(r,v_r) - \omega t + kz)}{(s\Omega\,(H,P_\theta,p_z) - \omega + kv_z)}. \qquad (76)$$

We are interested in calculating the power transferred from the electron beam to the cavity fields. Equation (70) for the TEM mode cavity electric field shows that the electric field has no azimuthal or axial components, so we only have to compute the radial component of the perturbed current in order to calculate the transferred power. Then

$$\mathbf{J}^1(r,\,\theta,\,z,\,t) = -e\int d^3p\; v_r\, f^1(\mathbf{r},\,\mathbf{p},\,t)\;\hat{r}\,, \qquad (77)$$

and the time averaged power loss of all of the electrons in the cavity, P, is therefore

$$P = -\,a\omega E_1 \int_0^{2\pi/\omega} dt \int_0^{L} dz \int_a^{b} r\,dr\;\frac{J_r^1(r,\,\theta,\,z,\,t)\,\sin\,(kz)\,\sin\,(\omega t)}{r}. \qquad (78)$$

Combining Equations (75), (77) and (78) we have

$$P = \frac{e^2 a^2 E_1^2}{4}\,\omega \sum_{s=1}^{\infty} \int_0^{2\pi/\omega} dt \sin(\omega t) \int_0^L dz \sin(kz) \int_a^b dr \int d^3p\, v_r$$

$$\left\{ \frac{\partial f^0(H, P_\theta, p_z)}{\partial H}\, a_s(H, P_\theta, p_z)\, (L_s(\omega, k) - L_s(\omega, -k) - L_s(-\omega, k) + L_s(-\omega, -k)) \right. \tag{79}$$

$$+ \left(\frac{1}{c} \frac{\partial f^0(H, P_\theta, p_z)}{\partial p_z} - \frac{v_z}{c} \frac{\partial f^0(H, P_\theta, p_z)}{\partial H} \right)$$

$$\left. a_s(H, P_\theta, p_z)(L_s(\omega,k) + L_s(\omega,-k) + L_s(-\omega,k) + L_s(-\omega,-k)) \right\}.$$

We now transform the integration over d^3p to an integration over $dH\, dP_\theta\, dp_z$ and perform the integration over r by the technique used between Equations (31) and (35) of Section II. This yields

$$P = \frac{e^2 a^2 E_1^2 \omega}{8} \sum_{s=1}^{\infty} \int_0^{2\pi/\omega} dt \sin(\omega t) \int_0^L dz \sin(kz) \int dH\, dP_\theta\, dp_z$$

$$\left\{ \frac{\partial f^0(H, P_\theta, p_z)}{\partial H}\, T(H, P_\theta, p_z)\, a_s^2(H, P_\theta, p_z)\, (G_s(\omega, k) - G_s(\omega, -k) - G_s(-\omega, k) + G_s(-\omega, -k)) \right. \tag{80}$$

$$+ \left(\frac{1}{c} \frac{\partial f^0(H, P_\theta, p_z)}{\partial p_z} - \frac{v_z}{c} \frac{\partial f^0(H, P_\theta, p_z)}{\partial H} \right)$$

$$\left. T(H, P_\theta, p_z)\, a_s^2(H, P_\theta, p_z)(G_s(\omega,k) + G_s(\omega,-k) + G_s(-\omega,k) + G_s(-\omega,-k)) \right\},$$

where

$$G_s(\omega, k) = \frac{\sin(\omega t + (s\Omega(H, P_\theta, p_z) - \omega)\, z/v_z) - \sin(\omega t - kz)}{(s\Omega(H, P_\theta, p_z) - \omega + kv_z)}. \tag{81}$$

Integrating over t and z we find the general expression for the power transferred from the electron beam to the cavity fields,

$$P = \frac{e^2 a^2 E_1^2 L}{8l} \sum_{s=1}^{\infty} \int dH\, dP_\theta\, dp_z$$

$$\left\{ \frac{\partial f^0(H, P_\theta, p_z)}{\partial H} T(H, P_\theta, p_z)\, a_s^2(H, P_\theta, p_z)\, (F_s(\omega, k) - F_s(\omega, -k) + F_s(-\omega, k) - F_s(-\omega, -k)) \right. \tag{82}$$

$$+ \left(\frac{1}{c} \frac{\partial f^0(H, P_\theta, p_z)}{\partial p_z} - \frac{v_z}{c} \frac{\partial f^0(H, P_\theta, p_z)}{\partial H} \right)$$

$$\left. T(H, P_\theta, p_z)\, a_s^2(H, P_\theta, p_z)\, (F_s(\omega, k) + F_s(\omega, -k) - F_s(-\omega, k) - F_s(-\omega, -k)) \right\},$$

where

$$F_s(\omega, k) = \frac{k^2 L^2\, (1 - \cos(kL) \cos((s\Omega(H, P_\theta, p_z) - \omega)\, L/v_z))}{(s\Omega(H, P_\theta, p_z) - \omega + k v_z) \left(k^2 L^2 - (s\Omega(H, P_\theta, p_z) - \omega)^2 \frac{L^2}{v_z^2} \right)}. \tag{83}$$

Equation (83) is a general expression for the beam power loss. In the next section we will specialize to an idealized distribution function which will allow the threshold beam power required for the cavity to self-oscillate to be easily calculated.

V. THE DISTRIBUTION FUNCTION OF THE ELECTRON BEAM

Before Equations (35) and (82) can be evaluated we must specify an equilibrium distribution function which is constructed from the constants of the motion, H, P_θ, and p_z. We choose the simplest distribution function possible which is that of a monoenergetic beam with one value of angular and axial momentum

$$f^0(\mathbf{r}, \mathbf{p}, t) = A\, \delta(H - H_0)\, \delta(P_\theta - P_{\theta_0})\, \delta(p_z - m v_0), \tag{84}$$

where A is determined from the condition

$$\frac{2\pi}{m} e \int_a^b r dr \int d^3p\, p_z f^0(\mathbf{r}, \mathbf{p}, t) = I, \tag{85}$$

and I is the negative of the current of electrons through the cavity. To evaluate the constant A in Equation (84) we insert Equation (84) into Equation (85) and transform the integration over d^3p into an integration over the constants of the motion. Then

$$I = \frac{2\pi Ae}{\sqrt{2m}} \int_a^b r dr \int \frac{dH\ dP_\theta\ dp_z\ p_z \delta(H - H_0)\ \delta\ (P_\theta - P_{\theta_0})\ \delta\ (p_z - m\mathrm{v}_0)}{r\sqrt{H - \frac{P_\theta^2}{2mr^2} - \frac{p_z^2}{2m} - P_0\ ln(\frac{r}{a})}}$$

$$= \sqrt{2m}\,\pi Ae\mathrm{v}_0 \int_{r_i}^{r_0} dr\ \frac{1}{\sqrt{H_0 - \frac{P_{\theta_0}^2}{2mr^2} - \frac{m\mathrm{v}_0^2}{2} - P_0\ ln(\frac{r}{a})}}. \tag{86}$$

Using Equation (36) for $T(H, P_\theta, p_z)$, the radial oscillation period of an electron with total energy H, angular momentum P_θ and axial momentum p_z, we see that Equation (86) can be written as

$$I = \pi T(H_0, P_{\theta_0}, m\mathrm{v}_0)\ e\mathrm{v}_0\ A. \tag{87}$$

Therefore, for an electron beam with energy H_0, current I, angular momentum P_{θ_0}, and axial momentum $m\mathrm{v}_0$, the distribution function is

$$f^0(H, P_\theta, p_z) = \frac{I}{\pi e\mathrm{v}_0 T(H_0, P_{\theta_0}, m\mathrm{v}_0)}\ \delta(H - H_0)\ \delta(P_\theta - P_{\theta_0})\ \delta(p_z - m\mathrm{v}_0)\,. \tag{88}$$

The distribution function given in Equation (88) is an idealized representation of the distribution function that would be present in an actual device. However, such a distribution function has many advantages from an analytical point of view. The principle advantage is that it allows for simple evaluation of the theory and yields results which are easily interpreted. The distribution function can also be used as the basis for superposing many solutions together to model the situation where the beam has arbitrarily spread in energy, angular momentum and axial momentum. The superposition principle is valid here because of the self-fields of the beam have been neglected and the theory is otherwise linear.

VI. RESULTS

The parameters we will use to describe the results of the linear theory of the orbitron traveling wave amplifier and oscillator are similar to the parameters used to describe the ECM. Indeed, the voltage between the center and outer conductor in an orbitron, V_0, plays the role of the magnetic field

in an ECM. The parameters H_0, the total electron energy; α, the square root of the ratio of the electron's perpendicular to parallel energy; and b, the radius of the inner surface of the waveguide or cavity outer conductor are also used for the ECM. Two parameters, the radius of the center conductor, a; and σ, the ratio of the maximum to the minimum radius of the electron's orbit, have no ECM analogy. The remaining eight quantities all have direct ECM counterparts. For the traveling wave amplifier we have the harmonic number, s; the electron beam current, I; the frequency, ω; and the spacial growth rate, k_i. The quality factor of the cavity, Q; the length of the cavity, L; the mode number, l; and the threshold beam power required for the cavity to self-oscillate, P_b^{th} are used for the oscillator. We hope that this comparison of parameters will help to clarify the results that we are about to present for those readers who are familiar with the ECM.

A. Traveling Wave Amplifier

1. Dispersion Relation

Combining Equation (35) for the dispersion relation with Equation (88) for the idealized beam distribution function, we obtain an explicit expression for the dispersion relation for a forward traveling wave in an axially uniform configuration

$$\left[k^2 - \frac{\omega^2}{c^2}\right] ln\left[\frac{b}{a}\right] = \frac{\mu_0 e^2 \omega}{4} \frac{I}{\pi e v_0 T(H_0, P_{\theta_0}, m v_0)} \sum_{s=1}^{\infty}$$

$$\left[1 - \frac{v_0}{c}\right] \frac{\partial}{\partial H} \left[T(H, P_{\theta_0}, m v_0)\, a_s^2 (H, P_{\theta_0}, m v_0) \left\{ \frac{1}{(s\Omega (H, P_{\theta_0}, m v_0) - \omega + k v_0)} \right.\right.$$

$$\left.\left. - \frac{1}{(s\Omega (H, P_{\theta_0}, m v_0) + \omega - k v_0)} \right\} \right]_{H = H_0} \qquad (89)$$

$$+ \frac{1}{c} \frac{\partial}{\partial p_z} \left[T(H_0, P_{\theta_0}, p_z)\, a_s^2 (H_0, P_{\theta_0}, p_z) \left\{ \frac{1}{(s\Omega (H_0, P_{\theta_0}, p_z) - \omega + k v_z)} \right.\right.$$

$$\left.\left. - \frac{1}{(s\Omega (H_0, P_{\theta_0}, p_z) + \omega - k v_z)} \right\} \right]_{p_z = m v_0}$$

Using Equations (43), (44), (67) and (69) for the derivatives of $T(H, P_\theta, p_z)$ and $a_s^2(H, P_\theta, p_z)$ developed in Section III and expressing the answer in terms of H_0, σ and α we obtain the final expression for the dispersion relation

$$\left[k^2 - \frac{\omega^2}{c^2}\right] = \frac{\mu_0 I \omega \Omega^2}{4\pi v_0 V_0} \sum_{s=1}^{\infty} \kappa_s^2(\sigma) \left\{ \left[\left[1 - \frac{2v_0}{c} \right] \frac{(2\kappa_s'(\sigma) - \eta(\sigma))}{(s\Omega - \omega + kv_0)} \right.\right.$$

$$\left. + \left[1 - \frac{2v_0}{c} \right] \frac{\eta(\sigma)\, s\Omega}{(s\Omega - \omega + kv_0)^2} - \frac{kv_0 P_0}{m v_0 c (s\Omega - \omega + kv_0)^2} \right] \tag{90}$$

$$- \left[\left[1 - \frac{2v_0}{c} \right] \frac{(2\kappa_s'(\sigma) - \eta(\sigma))}{(s\Omega + \omega - kv_0)} + \left[1 - \frac{2v_0}{c} \right] \frac{\eta(\sigma) s\Omega}{(s\Omega + \omega - kv_0)^2} \right.$$

$$\left.\left. + \frac{kv_0 P_0}{m v_0 c (s\Omega + \omega - kv_0)^2} \right] \right\}.$$

2. Spacial Growth Rate

The model we used to find the dispersion relation for the infinite length orbitron assumed that the electron beam interacted only with a forward traveling wave. In a real device, reflections at the output can cause a backward wave to be present in the interaction region. If the amplitude of the reflected signal reaches a level large enough for the loop gain of the system to exceed unity, the instability that gives rise to the maser interaction changes from convective to absolute and the amplifier self-oscillates. Internal feedback through coupling to the backward wave can also cause an absolute instability (Briggs, 1964). It is important to know the parametric dependences of the transition from convective to absolute instability when designing an actual device (Lau et al, 1981), and various schemes can be used to avoid the onset of an absolute instability such as lining the inner surface of the cavity with an absorbing material. Here, we choose to ignore the problem of absolute instability and simply solve Equation (90) to find the spacial growth rate for a forward traveling wave in an infinite length orbitron amplifier as a function of the frequency and beam parameters. It should be understood, however, that the growth rates that result may not be realized in an actual device due to the onset of an absolute instability.

Now, to solve Equation (90) for the spacial growth rate we assume that $\omega \cong s\Omega$ and that only the sth term is resonant in the infinite sum. Then Equation (90) can be written in a more tractable form,

$$\left[k^2-\frac{\omega^2}{c^2}\right](s\Omega-\omega+kv_0)^2=\frac{\mu_0\omega I\Omega^2\kappa_s^2(\sigma)}{4\pi v_0 V_0}$$

$$\left\{\left[1-\frac{2v_0}{c}\right](2\kappa_s'(\sigma)-\eta(\sigma))(s\Omega-\omega+kv_0)+\left[1-\frac{2v_0}{c}\right]\eta(\sigma)\,s\Omega-\frac{kv_0P_0}{mv_0c}\right\}. \tag{91}$$

Equation (91) is fourth order in k and has nine free parameters, a, b, α, σ, s, V_0, H_0, I and ω. In the numerical results that follow we reduce the number of free parameters by normalizing the radius of the center conductor, a, and the spacial growth rate, k_i, to the waveguide outer conductor radius b. We also normalize the frequency, ω, to the frequency c/b. We fix the value of α, which is the square root of the ratio of the perpendicular to parallel energy, at 1.5, which is a value typical of most ECM experiments (Chu, 1978). The parameter $\frac{b}{a}$ has been chosen to be 100; the harmonic number, s, is taken to be 1; the electron energy, H_0, is fixed at 10000 eV; and σ, the ratio of the maximum to the minimum radius of the electron's orbit, is taken to be 5. The three remaining parameters, V_0, the voltage between the center and outer conductor; I, the electron beam current; and the normalized frequency, $\frac{\omega c}{b}$, will be varied. Figure 8 plots the spacial growth rate versus frequency for $V_0 = 13500$ volts and $I = 100mA$. This is plotted over the lowest frequency interval that gives growth. The voltage chosen gives a maximum electron radius of about $.1b$. Thus the electron (with $\sigma = 5$) passes close to the center conductor yielding a large growth rate. Figure 9 plots the spacial growth rate versus the beam current for the value of V_0 used in Figure 8. The growth rate is seen to scale as $\sim I^{1/3}$. Last, the spacial growth rate is plotted versus V_0 in Figure 10 for the voltages that are consistent with radial confinement of the electrons. The beam current is taken to be 100 mA and the frequency was varied here and in Figure 9 to maximize the spacial growth rate.

B. Oscillator

1. Beam Power Transfer to the Cavity Fields

Combining Equations (82) and (88), we obtain an explicit expression for the power transferred from the electron beam to the cavity fields

$$P=-\frac{e^2a^2E_1^2L}{8l}\cdot\frac{I}{\pi e v_0 T(H_0,P_{\theta_0},mv_0)}\sum_{s=1}^{\infty}\left\{\frac{\partial}{\partial H}\left[T(H,P_{\theta_0},mv_0)\,a_s^2(H,P_{\theta_0},mv_0)\right.\right.$$

$$\left.\left.\left(F_s(\omega,k)-F_s(\omega,-k)+F_s(-\omega,k)-F_s(-\omega,-k)\right)\right]\right|_{H=H_0}$$

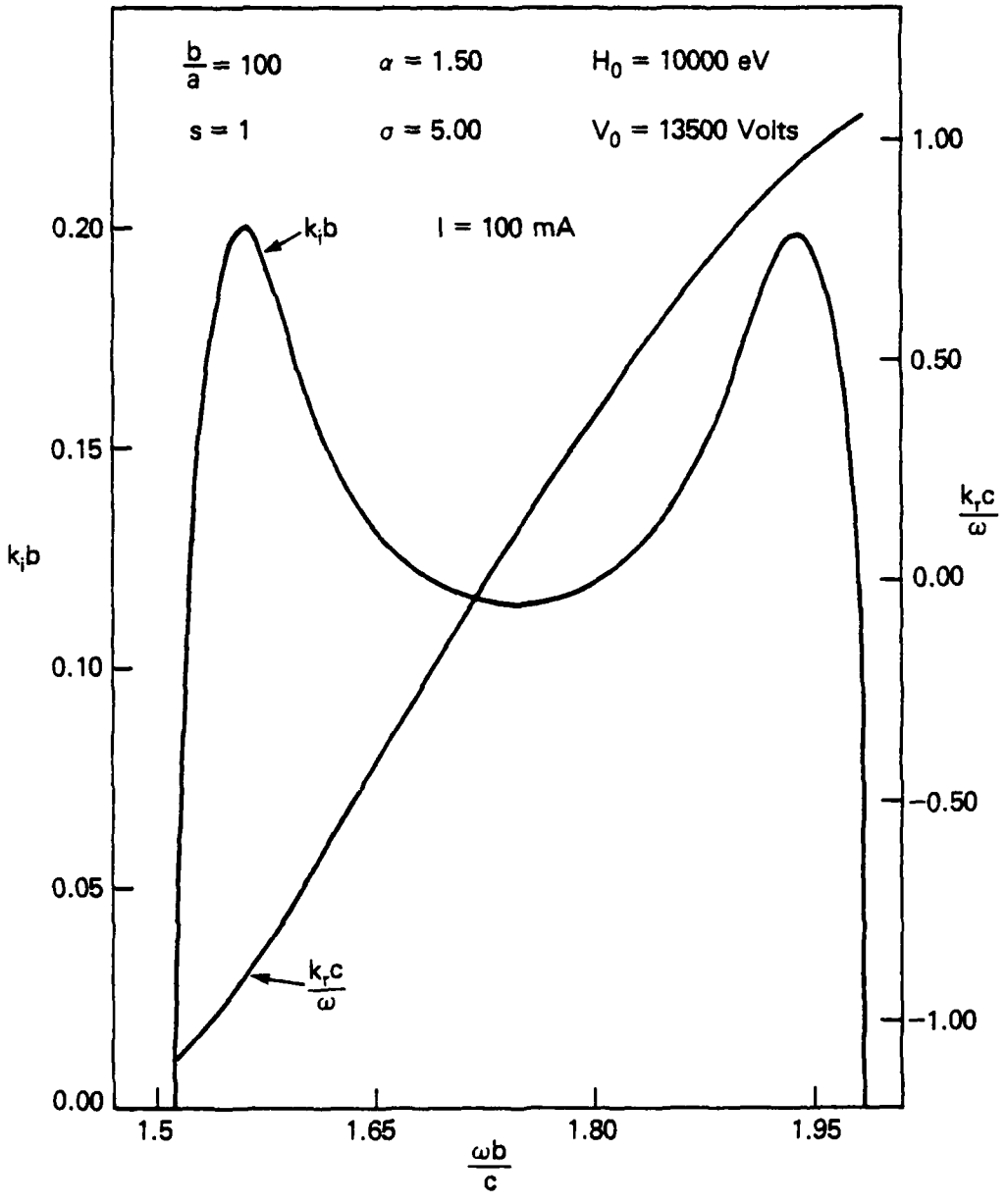

Figure 8. The spacial growth rate and wave number versus frequency for an orbitron traveling wave amplifier

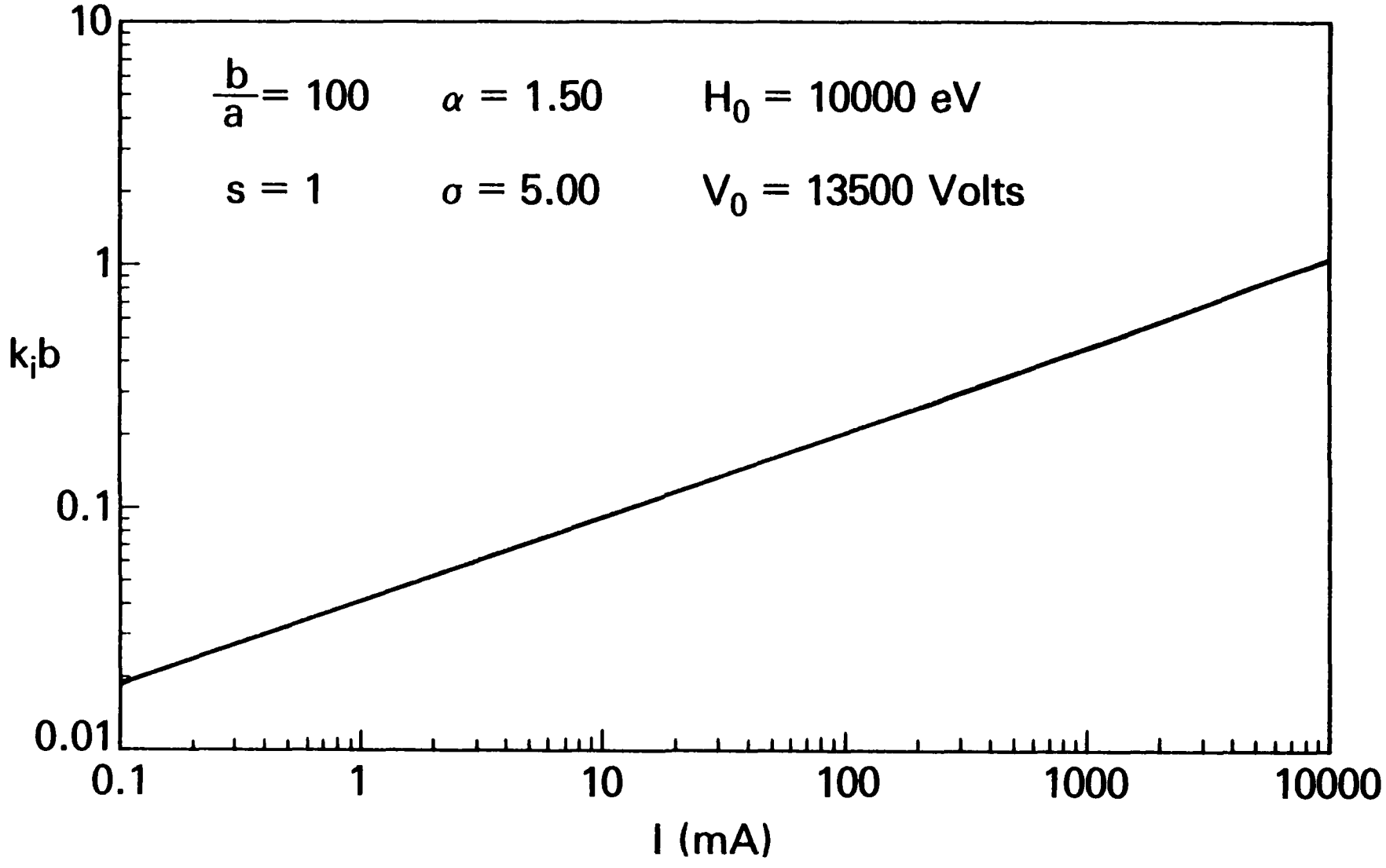

Figure 9. The spacial growth rate versus the electron beam current for an orbitron traveling wave amplifier

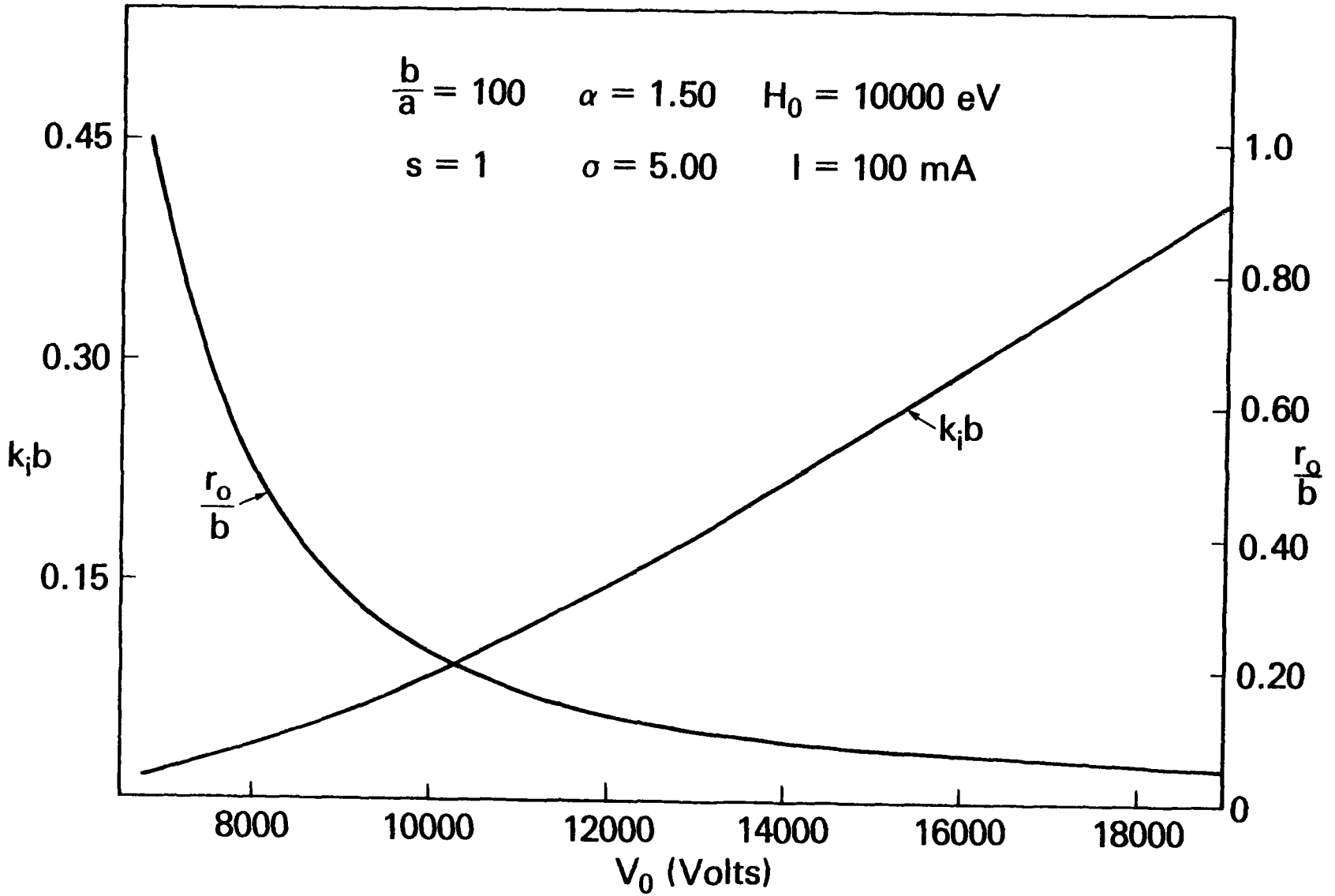

Figure 10. The spacial growth rate and the maximum electron radius versus the voltage between the center and outer conductor for an orbitron traveling wave amplifier

$$+\frac{1}{c}\frac{\partial}{\partial p_z}\Big[\, T(H_0, P_{\theta_0}, p_z)\; a_s^2(H_0, P_{\theta_0}, p_z) \tag{92}$$

$$\Big[F_s(\omega,k)+F_s(\omega,-k)-F_s(-\omega,k)-F_s(-\omega,-k)\Big]\Big]\Big|_{p_z=m\mathrm{v}_0}$$

$$-\frac{\mathrm{v}_0}{c}\frac{\partial}{\partial H}\Big[\, T(H, P_{\theta_0}, m\mathrm{v}_0)\; a_s^2(H, P_{\theta_0}, m\mathrm{v}_0)$$

$$\Big[F_s(\omega,k)+F_s(\omega,-k)-F_s(-\omega,k)-F_s(-\omega,-k)\Big]\Big]\Big|_{H=H_0},$$

where $F_s(\omega, k)$ is given by Equation (83). Using Equations (43), (44), (67) and (69) for the derivatives of $T(H, P_\theta, p_z)$ and $a_s^2(H, P_\theta, p_z)$ developed in Section III and expressing the answer in terms of H_0, σ, α, we obtain the final expression for the beam power loss,

$$P=\frac{\pi l a^2 ln\left(\frac{b}{a}\right) E_1^2\, I\, \Omega^2 \tau^2}{4V_0}\sum_{s=1}^{\infty}\kappa_s^2(\sigma)\Big\{P_s^1+P_s^2+P_s^3+P_s^4\Big\}, \tag{93}$$

where

$$P_s^1=\left[1-\frac{2\mathrm{v}_0}{c}\right](\eta(\sigma)-2\kappa_s'(\sigma))F(\Delta)+\eta(\sigma)\left[1-\frac{2\mathrm{v}_0}{c}\right]s\Omega\tau\, G(\Delta)-\frac{P_0}{m\mathrm{v}_0 c}H(\Delta), \tag{94}$$

$$P_s^2=-\left[1+\frac{2\mathrm{v}_0}{c}\right](\eta(\sigma)-2\kappa_s'(\sigma))L(\Delta)-\eta(\sigma)\left[1+\frac{2\mathrm{v}_0}{c}\right]s\Omega\tau\, M(\Delta)-\frac{P_0}{m\mathrm{v}_0 c}N(\Delta), \tag{95}$$

$$P_s^3=\left[1+\frac{2\mathrm{v}_0}{c}\right](\eta(\sigma)-2\kappa_s'(\sigma))F(\Delta)+\eta(\sigma)\left[1+\frac{2\mathrm{v}_0}{c}\right]s\Omega\tau\, G(\Delta)+\frac{P_0}{m\mathrm{v}_0 c}H(\Delta), \tag{96}$$

$$P_s^4=-\left[1-\frac{2\mathrm{v}_0}{c}\right](\eta(\sigma)-2\kappa_s'(\sigma))L(\Delta)-\eta(\sigma)\left[1-\frac{2\mathrm{v}_0}{c}\right]s\Omega\tau\, M(\Delta)+\frac{P_0}{m\mathrm{v}_0 c}N(\Delta), \tag{97}$$

$$F(\Delta)=-\frac{\sin^2\left(\frac{\Delta}{2}\right)}{\Delta^2(\Delta-2l\pi)}, \tag{98}$$

$$G(\Delta) = \frac{(3\Delta - 4l\pi)\sin^2\left(\frac{\Delta}{2}\right) - (\Delta - 2l\pi)\frac{\Delta}{2}\sin(\Delta)}{\Delta^3(\Delta - 2l\pi)^2}, \tag{99}$$

$$H(\Delta) = \frac{(\Delta^2 - 3\Delta l\pi + 2l^2\pi^2)\frac{\Delta}{2}\sin(\Delta) - (2\Delta^2 - 5l\pi\Delta + 4l^2\pi^2)\sin^2\left(\frac{\Delta}{2}\right)}{\Delta^3(\Delta - 2l\pi)^2}, \tag{100}$$

$$L(\Delta) = -\frac{\sin^2\left(\frac{\Delta}{2}\right)}{\Delta(\Delta - 2l\pi)^2}, \tag{101}$$

$$M(\Delta) = \frac{(3\Delta - 2l\pi)\sin^2\left(\frac{\Delta}{2}\right) - (\Delta - 2l\pi)\frac{\Delta}{2}\sin(\Delta)}{\Delta^2(\Delta - 2l\pi)^3}, \tag{102}$$

$$N(\Delta) = \frac{(\Delta - l\pi)(\Delta - 2l\pi)\frac{\Delta}{2}\sin(\Delta) - (2\Delta^2 - 3l\pi\Delta + 2l^2\pi^2)\sin^2\left(\frac{\Delta}{2}\right)}{\Delta^2(\Delta - 2l\pi)^3}, \tag{103}$$

$$\Delta = (s\Omega(H_0, P_{\theta_0}, mv_0) - \omega + kv_0)\tau, \tag{104}$$

$$\Delta' = (s\Omega(H_0, P_{\theta_0}, mv_0) + \omega + kv_0)\tau, \tag{105}$$

and

$$\tau = \frac{L}{v_0}. \tag{106}$$

2. Threshold Beam Power Required for Self-Oscillation

The model which we used to calculate the beam energy loss to the cavity fields assumed an idealized cavity with discrete eigenfrequencies. The cavity has a finite Q, however, and this implies that the cavity resonates in a narrow band of eigenfrequencies with a bandwidth of approximately $2\omega/Q$. It will

be shown in Section VII that the frequency width for beam energy loss to the cavity fields is approximately $2\pi/\tau$ and the finite Q cavity can therefore be treated as idealized if

$$\frac{\pi}{\tau} >> \frac{\omega}{Q}. \tag{107}$$

This condition is usually easily satisfied for any reasonable value of Q.

From the definition of Q,

$$Q = \frac{\omega\ E_s}{P_L}, \tag{108}$$

where E_s is the electromagnetic energy stored in the cavity and P_L is the electromagnetic power lost, we see that the threshold condition for oscillation occurs when the power lost from the cavity in the form of electromagnetic radiation is just balanced by the power input from the electron beam or

$$P \geqslant P_L, \tag{109}$$

which implies that

$$P > \frac{\omega\ E_s}{Q}. \tag{110}$$

Now, the beam power, P_b, is related to the beam current through the relation

$$P_b = H_0 I/e, \tag{111}$$

and the stored energy for a TEM mode in the cavity is given by

$$E_s = \frac{\pi}{2}\ \epsilon_0\ a^2\ E_1^2\ L\ ln\left(\frac{b}{a}\right). \tag{112}$$

Combining Equations (73), (93), (110), (111), and (112) yields the relation

$$P_b^{th} = \frac{2\pi\ \epsilon_0\ c\ V_0\ (H_0/e)}{Q\Omega^2\ \tau^2 \sum_{s=1}^{\infty} \kappa_s^2(\sigma)\ (P_s^1 + P_s^2 + P_s^3 + P_s^4)}. \tag{113}$$

Equation (113) is a function of nine free parameters, V_0, H_0, α, σ, b, a, L, l and Q. In the numerical examples that follow, we reduce the number of free parameters by normalizing the cavity length, L, and the radius of the center conductor, a, to the cavity outer conductor radius b. We take α to be 1.5 as we did in the numerical examples for the traveling wave amplifier. The parameter b/a has been chosen to be 100, and $\frac{L}{b}$ is taken to be 10. Finally, from Equation (113) we see that Q and P_b^{th} can be combined to form a single quantity, QP_b^{th}. The four remaining parameters V_0, the voltage between the center and outer conductors; H_0, the electron energy; σ, the ratio of the maximum to the minimum radius of the electron's orbit; and l, the mode number, will be varied. Figure 11 plots QP_b^{th} versus V_0 for $l = 1$, 2 and 5, $H_0 = 10000$ eV and $\sigma = 5$. This is plotted in the voltage range where the $s = 1$ interaction of the $l = 1$ mode occurs. The $l = 1$ interaction has the widest voltage tuning range and the largest QP_b^{th} for a given harmonic number, s. Figure 12 shows QP_b^{th} versus H_0 for $s = l = 1$, 2 and 5 and $\sigma = 5$. V_0 is varied here and in Figure 13, to minimize QP_b^{th}. The start power requirements for the lowest order mode are seen to increase rapidly as a function of the injection energy. Last, Figure 13 displays QP_b^{th} versus σ for $H_0 = 10000$ eV, $l = s = 1$, 2, 5, and $l = \frac{s}{2} = 1$, 2. QP_b^{th} is seen to decrease as σ increases with saturation occurring when $\sigma \sim 5\,\frac{s}{l}$.

VII. DISCUSSION

A. Consistency of Approximations

We wish to verify that the assumptions we made in Section II are consistent with the results of the calculations performed in Sections II and IV. First, we consider assumption (ii), the requirement that the electric field due to the electron beam is small compared to the confining electric field due to the voltage between the inner and outer surfaces of the waveguide. Now, the electric field of the azimuthally symmetric electron beam is largest compared to the confining electric field for radii greater than the maximum radius of the electron beam, r_o. Therefore, we have the relation

$$\frac{I}{2\pi\epsilon_0 v_0 r_o} << \frac{V_0}{\ln\left(\frac{b}{a}\right) r_o}. \tag{114}$$

For the examples presented in Section VI, $v_0 \approx .1c$, $V_0 \approx 10{,}000$ volts and $\frac{b}{a} = 100$ for which Equation (114) yields

$$I << 3.6 \text{ amperes}, \tag{115}$$

and this is easily satisfied.

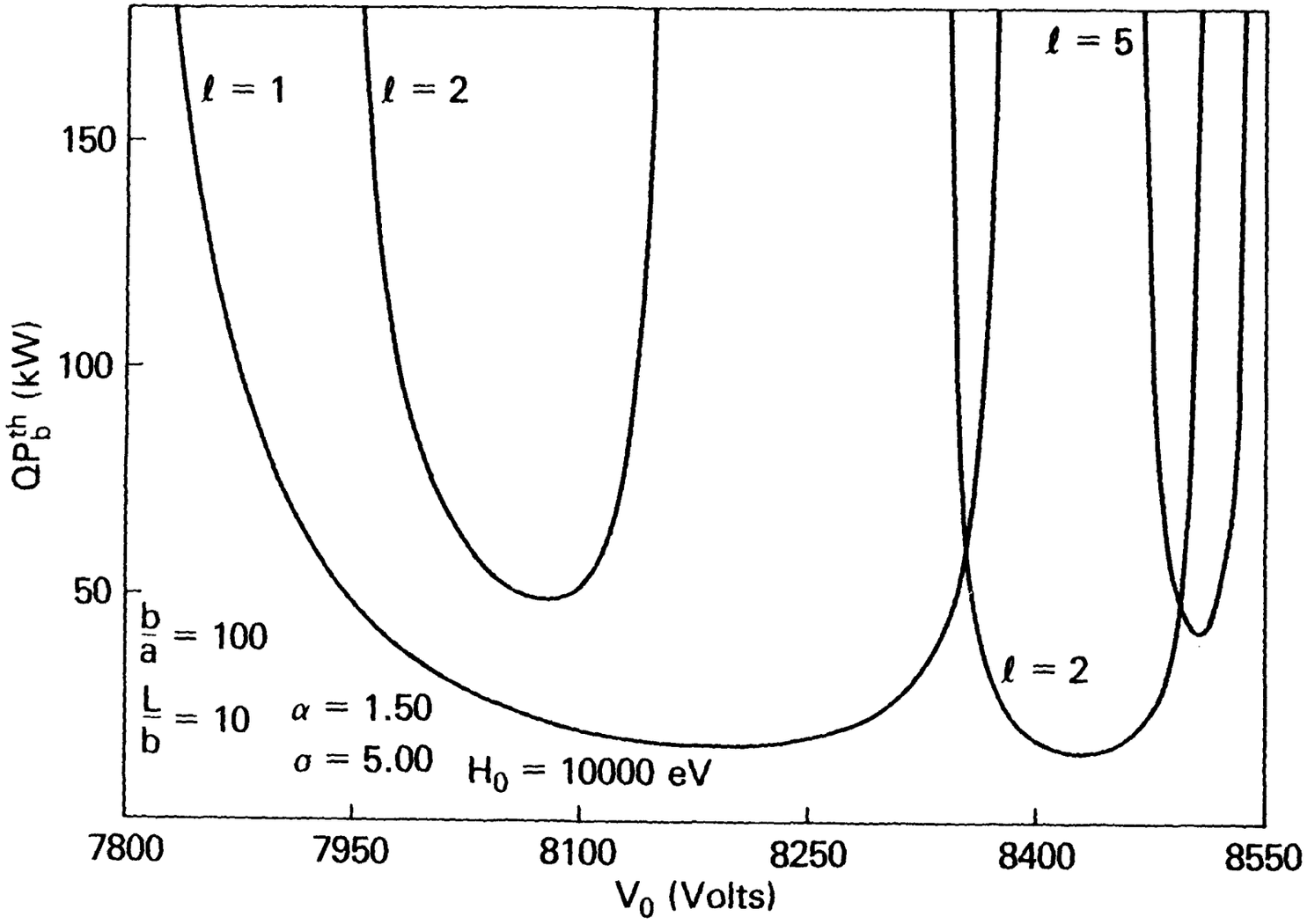

Figure 11. The cavity Q multiplied by the threshold beam power required for self-oscillation versus the the voltage between the center and outer conductor for various mode numbers in an orbitron oscillator

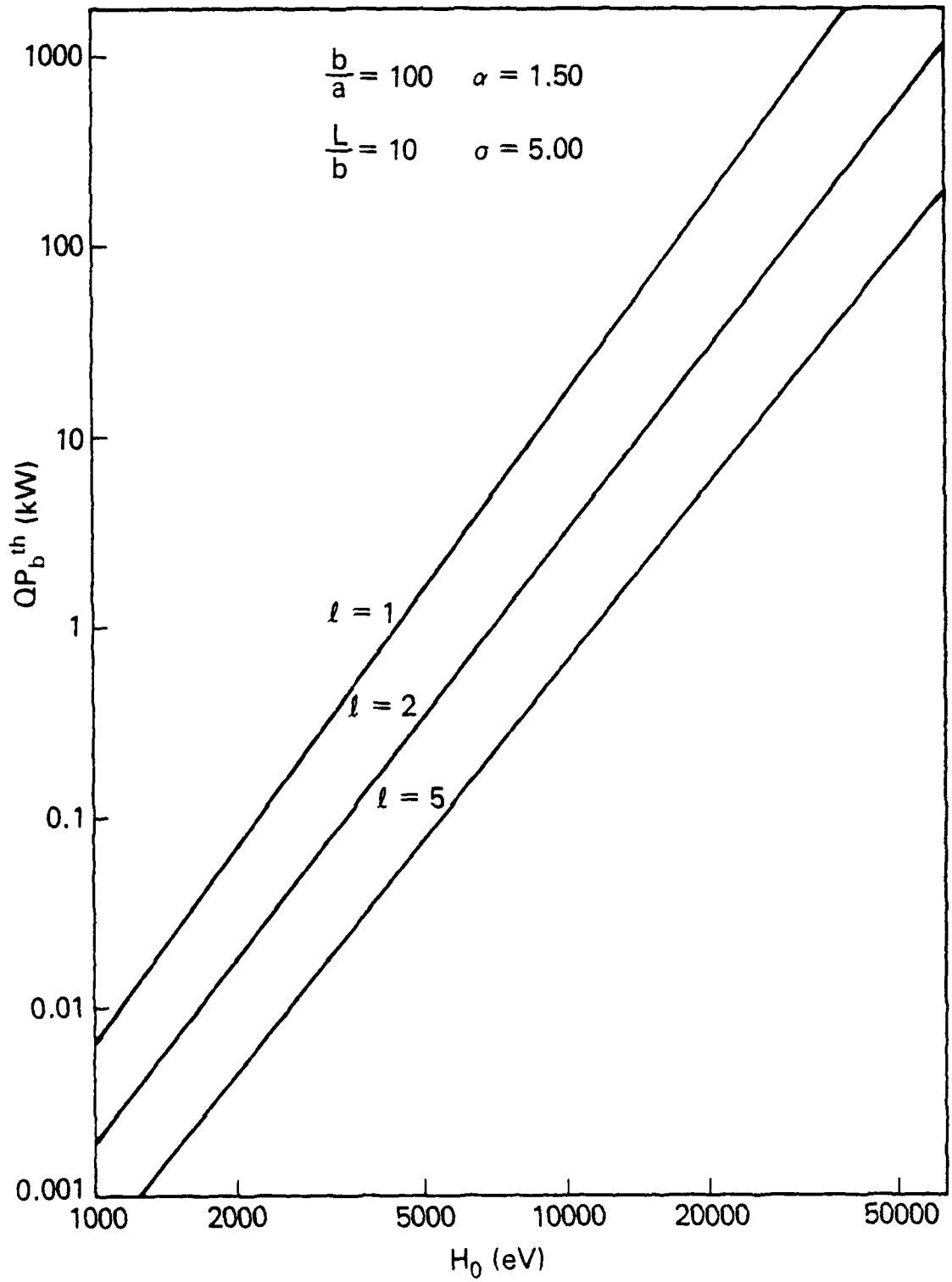

Figure 12. The cavity Q multiplied by the threshold beam power required for self-oscillation versus the electron beam energy for various mode numbers in an orbitron oscillator

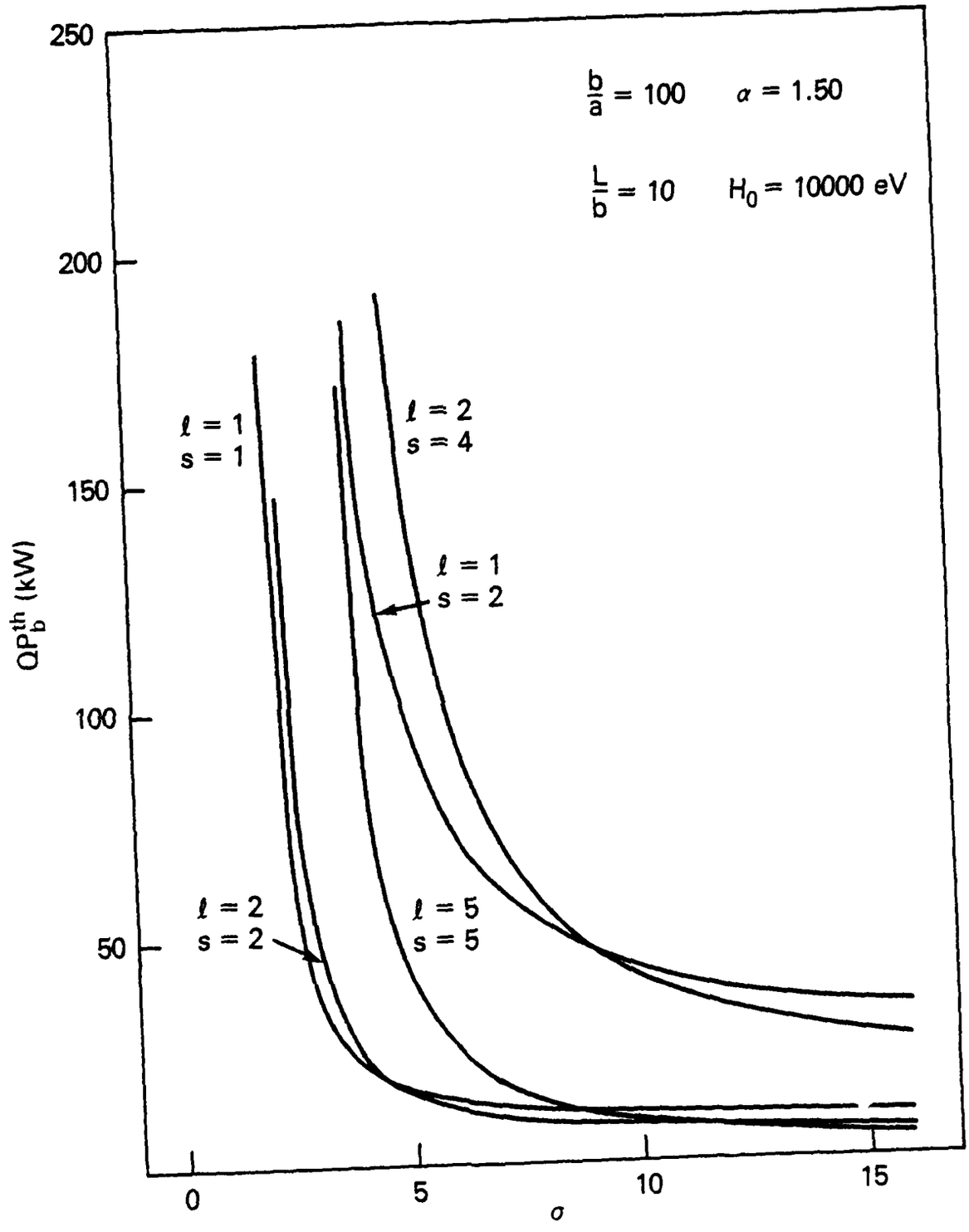

Figure 13. The cavity Q multiplied by the threshold beam power required for self-oscillation versus the parameter σ for various mode and harmonic numbers in an orbitron oscillator

Next, to verify the validity of assumption (iii) of Section II, we must show that the amplitude of the radiation electric field in the interaction region, E_1, is small compared to the confining electric field, that is

$$\frac{a}{r} E_1 << \frac{V_0}{\ln\left(\frac{b}{a}\right) r}. \tag{116}$$

We choose to verify that Equation (116) is valid for the oscillator configuration which has a larger radiation electric field amplitude in the interaction region than the amplifier configuration for a given output power. Writing Equation (116) in terms of the output power using Equations (108) and (112), we have

$$QP_L << l \frac{\pi^2 c \epsilon_0}{2} \frac{V_0^2}{\ln\left(\frac{b}{a}\right)}. \tag{117}$$

In the example shown in Figure 11 where $QP_b^{th} = 17$ kW for $V_0 \cong 8200$ volts, $\frac{b}{a} = 100$ and $l = 1$ we find from Equation (117) that

$$QP_L << 191 \text{ kW}. \tag{118}$$

Therefore, the threshold value of the beam power required for self-oscillation is less that one tenth the output power needed to violate Equation (116) and assumption (iii) is seen to be easily satisfied.

B. Frequency Bandwidth of the Interaction and Allowable Beam Spread for the Oscillator Configuration

To investigate the frequency bandwidth of the orbitron maser interaction in the oscillator configuration, we plot the beam energy transferred to the cavity radiation fields versus the parameter Δ for the $l = 1$ and $l = 2$ modes in Figures 14 and 15. It can be seen that the range of Δ for beam energy loss to the cavity radiation fields is roughly 2π. The frequency bandwidth of the interaction is therefore $2\pi/\tau$. This allows us to compute the allowable spread in the beam parameters to insure that the cold beam distribution function given in Section V is valid. Now, we have

$$(s\delta\Omega - \omega + k\delta v_0) << \frac{2\pi}{\tau}, \tag{119}$$

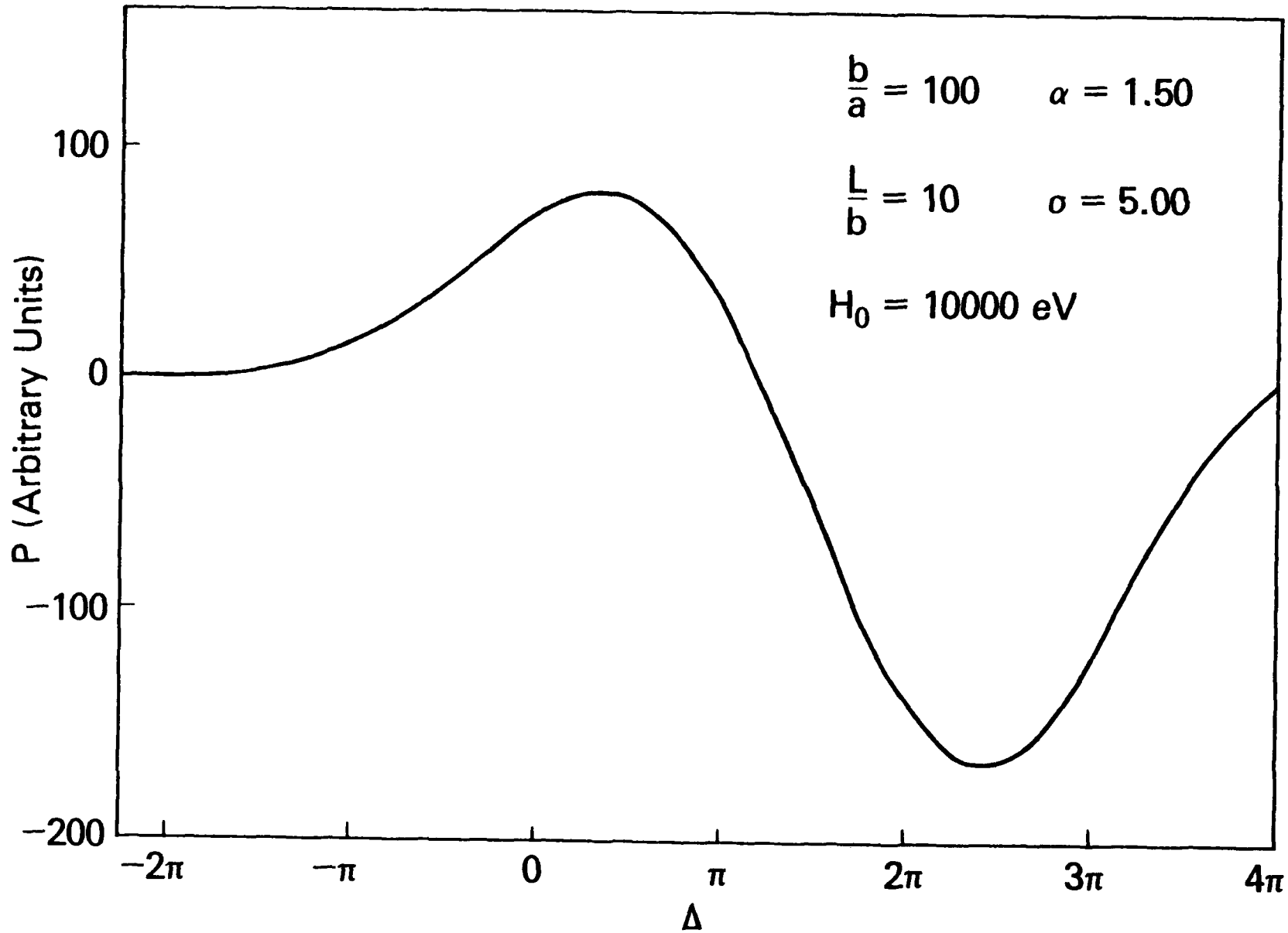

Figure 14. The electron beam power transferred to the radiation fields versus the parameter Δ for $l = 1$, $s = 1$.

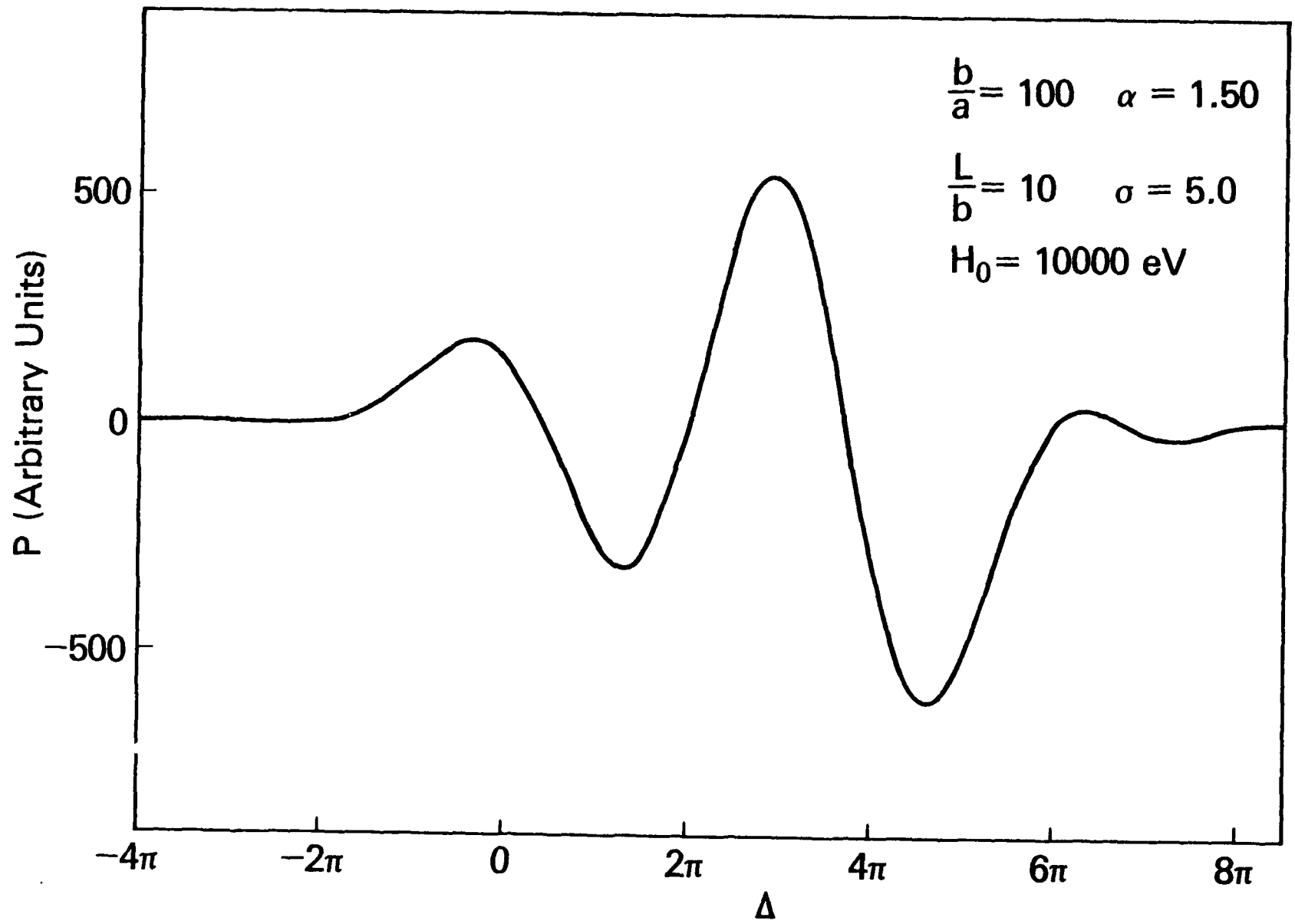

Figure 15. The electron beam power transferred to the radiation fields versus the parameter Δ for $l = 2$, $s = 1$.

and this implies that

$$\frac{\delta\Omega}{\Omega} << \frac{2\pi}{s\Omega\tau} << \frac{1}{sN}, \tag{120}$$

where N is the number of turns the electron makes around the central conductor while transiting the cavity. We also have a condition on the spread in v_z,

$$\frac{\delta v_z}{v_z} << \frac{2\pi}{k v_0 \tau}, \tag{121}$$

and, using Equations (72) and (106), we find that

$$\frac{\delta v_z}{v_z} << \frac{2}{l}. \tag{122}$$

We can write Equations (120) and (122) in terms of the allowable spread in the beam parameters H, σ and α by using Equations (43), (46), and (50),

$$\eta(\sigma)\ \frac{\delta H}{P_0} << \frac{1}{sN}, \tag{123}$$

$$\frac{2\alpha}{(1+\alpha^2)^2}\ \frac{H}{P_0}\ \delta\alpha << \frac{1}{sN}, \tag{124}$$

$$\frac{\alpha\ \delta\alpha}{(1+\alpha^2)} << \frac{2}{l}, \tag{125}$$

and

$$\frac{\frac{\partial \hat{T}(\sigma)}{\partial\sigma}}{\hat{T}(\sigma)}\ \delta\sigma << \frac{1}{sN}, \tag{126}$$

where $\partial \hat{T} / \partial\sigma$ is the derivative of the curve shown in Figure 5.

For a numerical example of the allowable spread in the beam parameters we use the $l = 2$ mode with the lowest threshold beam power shown in Figure 11. The value of sN is about 9 in this case. Using Equations (123) - (126) with the parameters of Figure 11 we find that

$$\frac{\delta H}{H} << .02, \tag{127}$$

$$\frac{\delta \sigma}{\sigma} << 3.7, \tag{128}$$

and

$$\frac{\delta \alpha}{\alpha} << .05. \tag{129}$$

The conditions on H and σ seem to be easily achievable; however, the allowable spread in the parameter α could pose a problem. Any effort to design an electron gun for a TEM orbitron oscillator should pay close attention to the spread in the beam parameters.

C. Nonlinear Efficiency Limits

Here we consider the maximum energy that can be transferred from the electron beam to a TEM waveguide mode in an orbitron. Since the electric field of a TEM mode has only a radial component, the angular momentum of an electron that interacts with this mode is conserved. Also, the electron has given the maximum amount of energy to the TEM mode if it exits the interaction region with no radial velocity. Therefore, to compute an upper bound on the power transfer from the electron beam to the TEM mode, we calculate the change in energy of electrons that enter the interaction region with energy H_0 having nonzero radial velocity and exit it with energy H^* having no radial velocity, consistent with the axial velocity change of the electrons due to the interaction with the TEM mode.

We consider the case of a forward traveling wave amplifier. The analysis is also valid for the oscillator configuration if the electron beam interacts primarily with the forward wave component of the standing wave in the cavity. (If the electron beam interacts principally with the backward wave in the cavity, the analysis is performed with the right hand side of Equation (130) having the opposite sign.) Now, from Equations (13) and (14) we see that the only nonzero components of the TEM waveguide mode are E_r and B_θ and

$$E_r = cB_\theta. \tag{130}$$

The equations of motion are then

$$\frac{dH}{dt} = -ev_r E_r, \tag{131}$$

and

$$\frac{dp_z}{dt} = -\, ev_r B_\theta , \tag{132}$$

and combining Equations (130), (131) and (132), we find that

$$\frac{dH}{dt} = c\, \frac{d}{dt}\, p_z . \tag{133}$$

This implies that $H - cp_z$ is a constant of the motion for electrons that transit interaction region.

Now, the Hamiltonian of an electron entering the interaction region is given by

$$H_0 = \frac{p_r^2}{2m} + \frac{p_z^2}{2m} + \Psi(r) , \tag{134}$$

where $\Psi(r)$ is an equivalent potential

$$\Psi(r) = \frac{P_\theta^2}{2mr^2} + P_0 \ln\left(\frac{r}{a}\right) . \tag{135}$$

The function $\Psi(r)$ is a monotonically decreasing function of r for $a \leqslant r < r^*$ and is a monotonically increasing function of r for $b \geqslant r > r^*$. A schematic plot of $\Psi(r)$ is given in Figure 16. In this figure $H_\perp$, where

$$H_\perp = H_0 - \frac{p_z^2}{2m} , \tag{136}$$

denotes the perpendicular energy of an electron entering the interaction region and r_i and r_o are the minimum and maximum radial position of an electron with perpendicular energy $H_\perp$. For the electron to exit the interaction region with minimum perpendicular energy it must have radial position r^* and no radial velocity. To compute the value of r^* we find the radial position of the minimum of $\Psi(r)$, using the relation

$$\left.\frac{\partial \Psi(r)}{\partial r}\right|_{r=r^*} = 0 . \tag{137}$$

This yields

$$r^* = \frac{P_\theta}{\sqrt{mP_0}} . \tag{138}$$

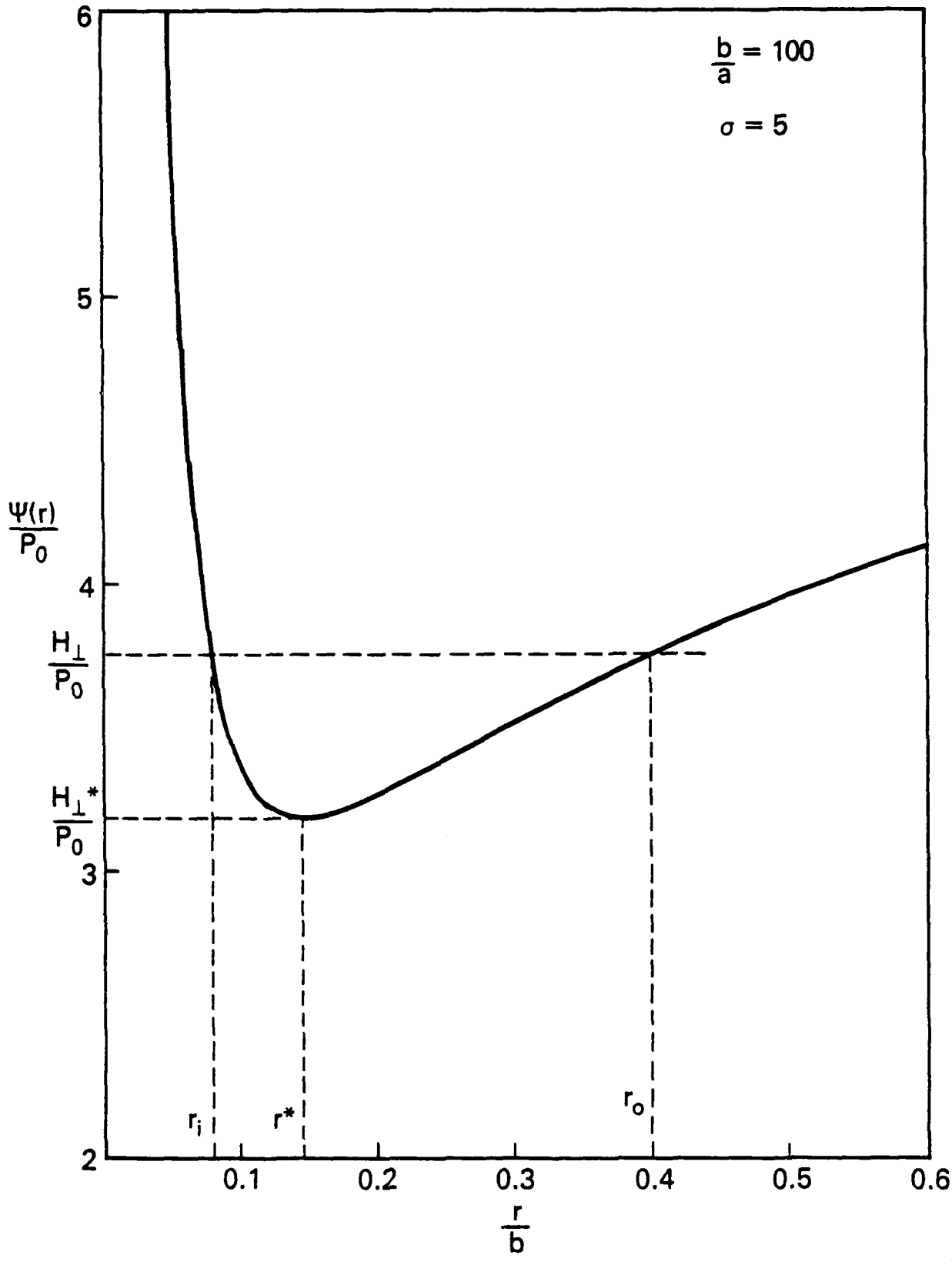

Figure 16. The equivalent potential of an electron orbiting the center conductor of an orbitron.

Now, writing the angular momentum, parallel energy, and the Hamiltonian in terms of the parameters r_o, σ and α defined in Section III, we have

$$P_\theta = r_o \sqrt{\frac{2mP_0\ln(\sigma)}{\sigma^2 - 1}}, \tag{139}$$

$$H_{||} = \frac{p_z^2}{2m} \tag{140}$$

$$= \frac{H_0}{1+\alpha^2},$$

and

$$H_0 = \left(\frac{1+\alpha^2}{\alpha^2}\right)\left[P_0 \ln\left(\frac{r_o}{a}\right) + P_0 \frac{\ln(\sigma)}{\sigma^2 - 1}\right]. \tag{141}$$

Then using Equations (134), (135), (138), (139) and (140), we find that the minimum energy of an electron exiting the interaction region is given by

$$H^* = \frac{P_0}{2} + P_0 \ln\left(\frac{r_o}{a}\right) + \frac{P_0}{2}\ln\left(\frac{2\ln(\sigma)}{\sigma^2 - 1}\right) + H_{||}^*, \tag{142}$$

where $H_{||}^*$ is determined from using the constant of the motion in the interaction region, $H - cp_z$, and Equation (140),

$$H^* - c\sqrt{2mH_{||}^*} = H_0 - c\sqrt{\frac{2mH_0}{(1+\alpha^2)}}. \tag{143}$$

We combine Equations (141), (142) and (143) to find the maximum energy that an electron can transfer to the TEM waveguide mode,

$$H_0 - H^* = \frac{P_0}{2} \frac{\left[\frac{2\ln(\sigma)}{\sigma^2 - 1} - 1 - \ln\left[\frac{2\ln(\sigma)}{\sigma^2 - 1}\right]\right]}{\left[1 - \sqrt{\frac{2H_0}{mc^2(1+\alpha^2)}}\right]}, \tag{144}$$

to lowest order in $(H_0 - H^*)/mc^2$.

If the electron beam current through the interaction region is I, Equation (144) implies a theoretical limit to the radiation power output of a TEM orbitron maser

$$P_{Max} = \frac{IV_0}{2\ln\left(\frac{b}{a}\right)} \frac{\left[\frac{2\ln(\sigma)}{\sigma^2-1} - 1 - \ln\left(\frac{2\ln(\sigma)}{\sigma^2-1}\right)\right]}{\left[1 - \sqrt{\frac{2H_0}{mc^2(1+\alpha^2)}}\right]}. \tag{145}$$

Similarly, the theoretical limit to the radiation efficiency, $\mathscr{E}_{Max}$, is given by

$$\mathscr{E}_{Max} = \frac{P_0}{2H_0} \frac{\left[\frac{2\ln(\sigma)}{\sigma^2-1} - 1 - \ln\left(\frac{2\ln(\sigma)}{\sigma^2-1}\right)\right]}{\left[1 - \sqrt{\frac{2H_0}{mc^2(1+\alpha^2)}}\right]}. \tag{146}$$

D. Mode Selection

The TEM mode is the lowest order mode of a coaxial cavity. It has large electric fields near the center conductor which is an advantage for operation at high harmonics of the radial oscillation frequency. However, unlike the TE modes, the TEM mode has the disadvantage that it has no cutoff frequency. The cavity outer wall radius cannot be reduced below the cutoff radius to provide a strong reflection of the forward or backward wave that makes up the standing wave in the cavity.

We can use two methods to provide reflection at the entrance or exit regions of the cavity at the desired operation frequency. One method is to modulate the outer cavity wall with a periodicity λ_w. Fortunately, we see from the results of the discussion of the maximum possible efficiency of the TEM orbitron in Part C that the efficiency of the device is maximized when the voltage V_0 is maximized. This implies that the maximum radius of the electrons orbit, r_0, is minimized for high efficiency operation. We can therefore have large ripples in the outer wall of the cavity without intercepting the electron beam while operating in the high efficiency regime of the device. The other scheme involves periodically placing azimuthally symmetric conducting breaks at the radius of the cavity outer conductor with radial waveguides extending into the insulator. The radial waveguide sections would be tuned to provide an optimal cavity Q at the desired operating frequency and minimal cavity Q at unwanted frequencies. This scheme has the advantage that it will not strongly cut off TE modes producing a large cavity Q for an unwanted mode. It also has the added feature that conducting breaks are required in any case to increase the potential of the outer conductor from its large negative value in the interaction region to a small negative or ground potential in the collector region. Last, we should mention that all

TE modes produce azimuthal currents in the cavity outer conductor and TEM modes have no azimuthal wall currents. Lossy material can therefore be incorporated into the cavity design to dissipate azimuthal currents and therefore lower the value of Q for a TE mode while having a small effect on cavity Q for a TEM mode.

A conceptual design of a TEM orbitron cavity is shown in Figure 17. Further analysis is required to find the shape and number of ripples in the cavity outer wall and the spacing and length of the radial waveguides to provide optimal reflection at a given operating frequency.

E. Beam Formation

We envision forming an azimuthally symmetric electron beam in accordance with assumption (i) of Section II. The electrons would be emitted from an azimuthally symmetric tungsten dispenser cathode through a grid into the beam injection region as shown in Figure 18. The electrons would be injected with a large value of axial momentum, a small value of radial momentum and, of course, no angular momentum due to the azimuthal symmetry. The angular momentum would be created and controlled by the presence of a weak azimuthally symmetric magnet field. As an illustration we assume that the magnetic vector potential of the applied field is given by

$$\mathbf{A}(r,z) = \frac{rB_0}{2}\,\hat{\theta}, \tag{147}$$

in the beam formation region. The canonical angular momentum of the injected electrons would then be

$$P_\theta = \frac{-er_e^2}{2}\,B_0, \tag{148}$$

where r_e is the radius of the grid. The magnetic field would be shielded out of the beam compression region and the interaction region by the presence of an iron shield which surrounds the downstream portion of the device to remove the injection magnetic fields and any other stray magnetic field that are present. The electrons then enter the beam compression region with the value of angular momentum given by Equation (148) even though the field has been removed. To find the magnitude of the magnetic field required in the beam injection region, we use Equations (139) and (148)

$$B_0 = -\frac{2\,r_o}{e\,r_e^2}\sqrt{\frac{2mP_0\ln(\sigma)}{\sigma^2-1}}, \tag{149}$$

and for $V_0 = 10000$ volts, $b/a = 100$, $\sigma = 5$, $r_o = 1$ mm and $r_e = 1$ cm we find that $B_0 = 8.1$ gauss.

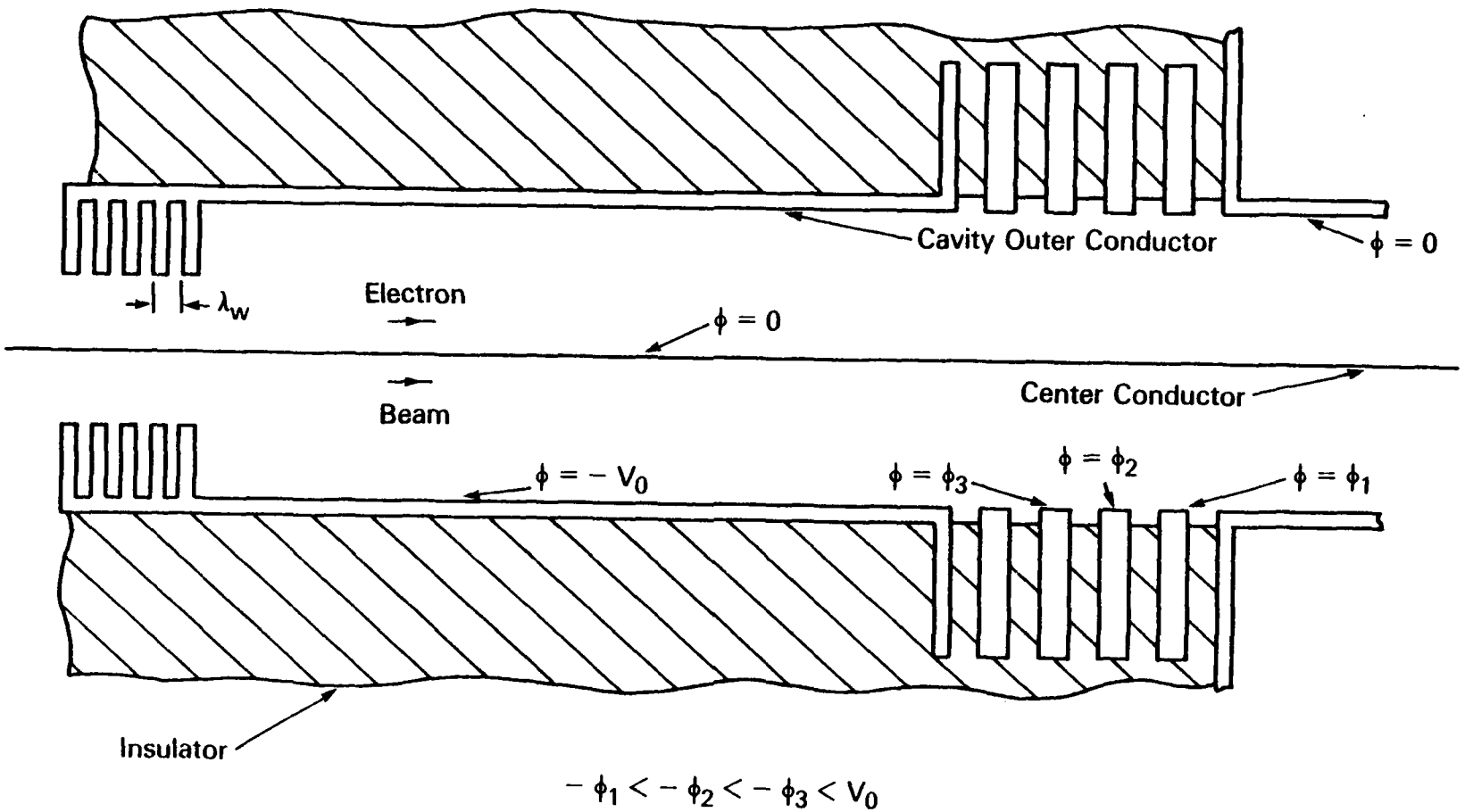

Figure 17. A conceptual design of a TEM orbitron cavity.

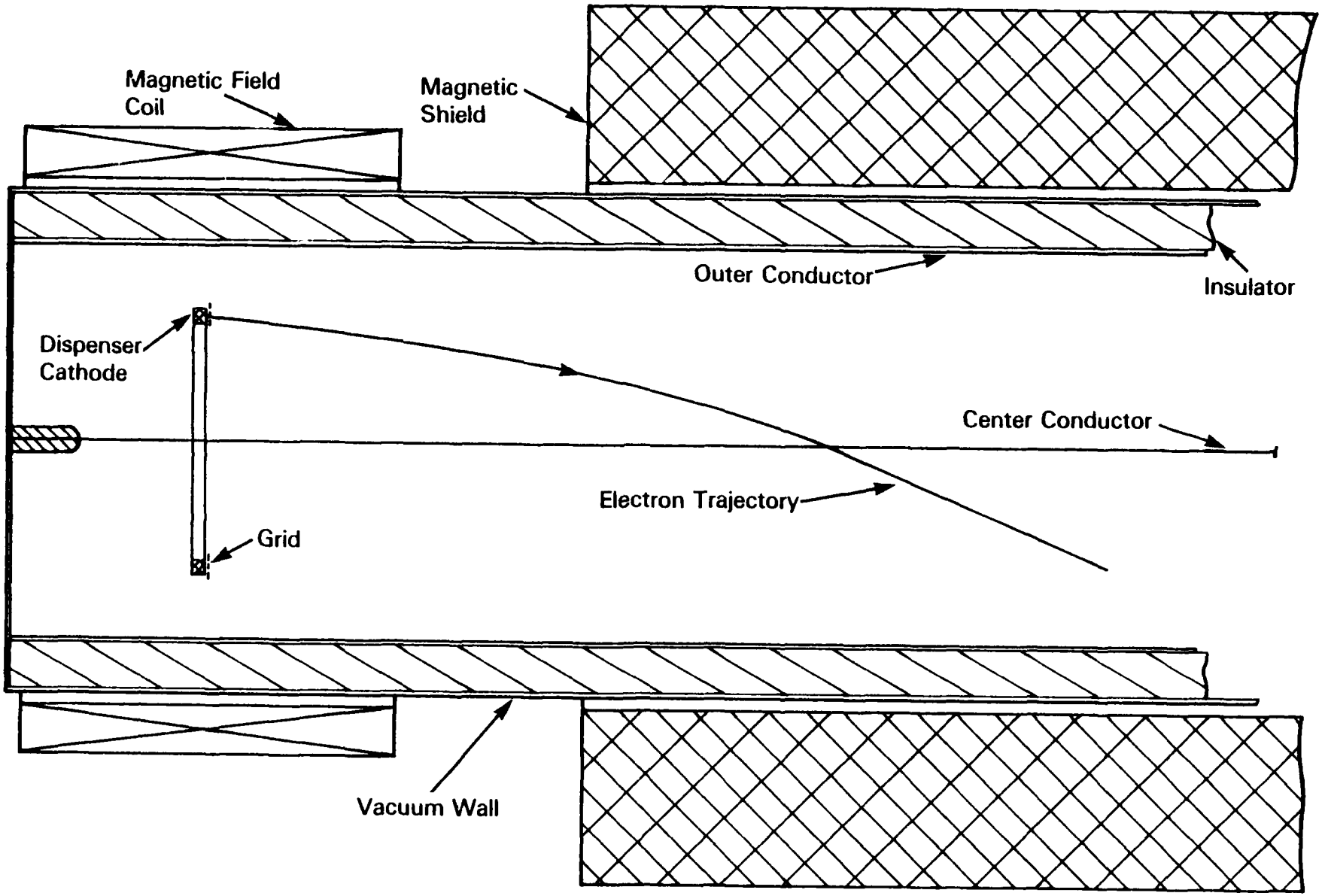

Figure 18. A conceptual design of the beam injection region of an axial injection orbitron.

An alternative to the above injection scheme is to use a non-azimuthally symmetric cathode and grid structure shaped similar to a turbine to inject the beam. This scheme has the advantage that it does not require a magnetic field to give the beam angular momentum. The beam would not be completely azimuthally symmetric, however, and the ability to independently control the two beam parameters σ and α would be lost. It might be advantageous to use this type of injection scheme in a production device, once the optimal beam parameters become known.

The beam exits the injection region and enters the compression region as shown in Figure 19. Here the beam is adiabatically compressed so that it enters the interaction region with a small axial momentum and a small maximum radius. If the beam is adiabatically compressed the value of the radial action, S, where

$$S = \oint p_r \, dr \,, \tag{150}$$

is invariant. Evaluating Equations (150) using Equation (5), (37), (38), (39) and (42), we find that

$$S = P_\theta \int_{\xi_o}^{\xi_i} \frac{d\xi}{\xi^2} \sqrt{\beta + \ln(\xi) - \xi^2} \,. \tag{151}$$

P_θ is conserved since the compression region is azimuthally symmetric. Therefore the parameter β is an adiabatic invariant because the integral is solely a function of β. We see from Equation (48) that σ is therefore also an adiabatic invariant. Now, using the fact that the parameters H_0, σ, β and P_θ are invariant in the beam compression region, we can use Equations (3), (39), (139) and (140) to find two equations that relate the parameters a, b, r_0, V_0 and α in the interaction region to their values as they exit the injection region, a', b', r_0', V_0' and α',

$$r_o \sqrt{P_0} = r_o' \sqrt{P_0'}, \tag{152}$$

and

$$\frac{\alpha^2}{(1+\alpha^2)} \frac{P_0'}{P_0} + \frac{P_0'}{H_0} \ln\left(\frac{\sqrt{P_0}\, a}{\sqrt{P_0'}\, a'}\right) = \frac{\alpha'^2}{(1+\alpha'^2)} \,, \tag{153}$$

$$\text{where} \quad P_0' = \frac{eV_0'}{\ln\left(\dfrac{b'}{a'}\right)} \,. \tag{154}$$

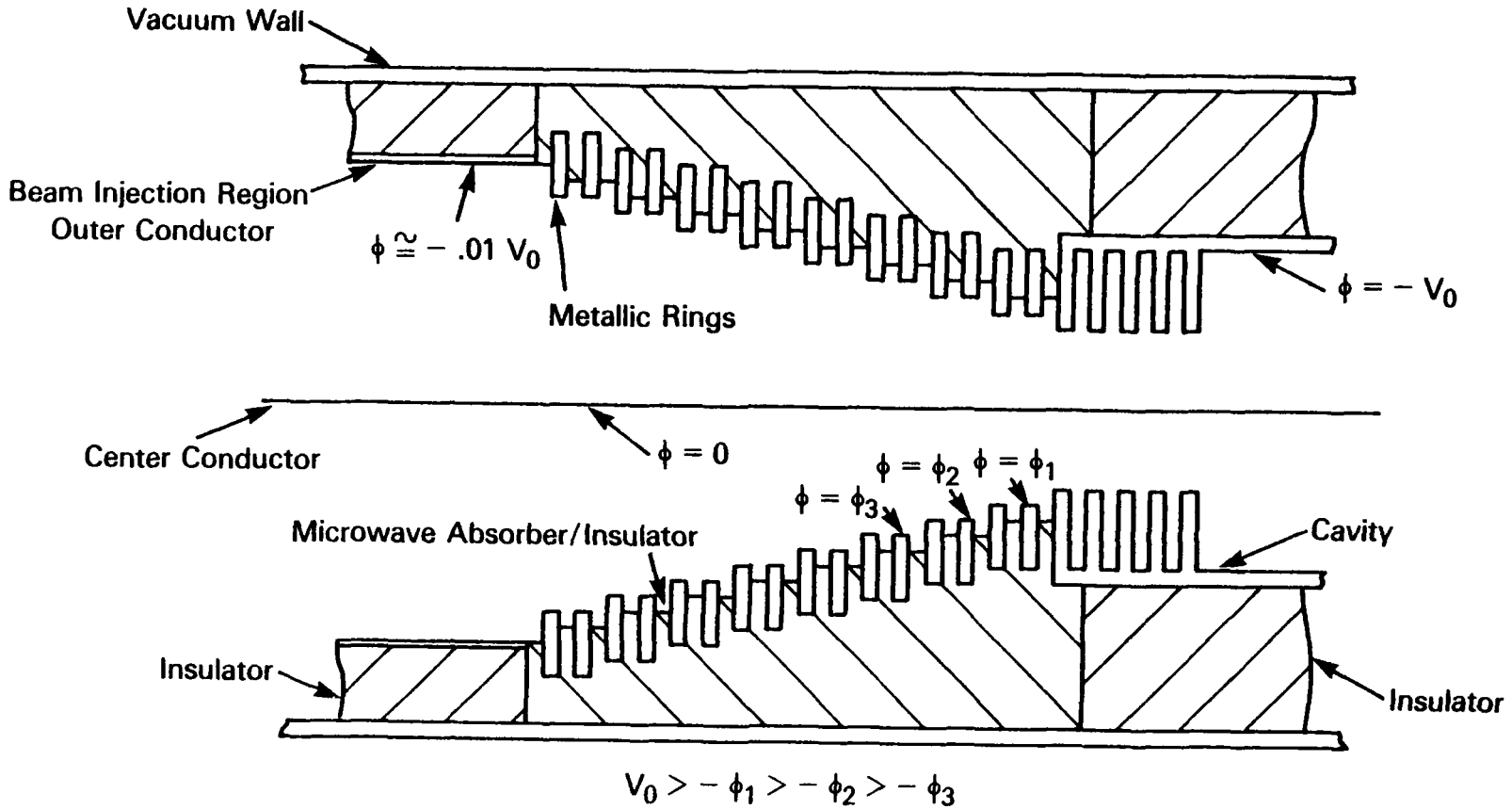

Figure 19. A conceptual design of the beam compression region in an axial injection orbitron.

For a numerical example of the design equations for an adiabatically compressed beam we will calculate P'_0 and α' for the interaction region parameters of Figure 8 and $a' = a$, $b' = 1.5b$ and a compression ratio of 10. Now, using Equations (3) and (152) we find that

$$V'_0 = 146.9 \text{ volts}, \tag{155}$$

and inserting this value of V'_0 into Equation (153) yields the value of α required at the entrance to the beam compression region, that is

$$\alpha' = ..18. \tag{156}$$

Finally, a conceptual design of a TEM orbitron oscillator is shown in Figure 20.

VIII. CONCLUSIONS

In this paper we have presented the linear theory of the TEM orbitron maser, and gained an understanding of the basic operation of the device in both the oscillator and traveling wave amplifier configurations. There appears to be great promise in developing the concept of an axial injection TEM orbitron maser as an inexpensive, high efficiency source of high frequency microwave radiation.

Further work is required in the area of mode selectivity in the cavity and in the details of the electron injection scheme. The linear theory of the TE mode must also be worked out to quantify the problem of TE mode competition with the TEM mode. Hopefully this will occur in the near future and a prototype device will be constructed.

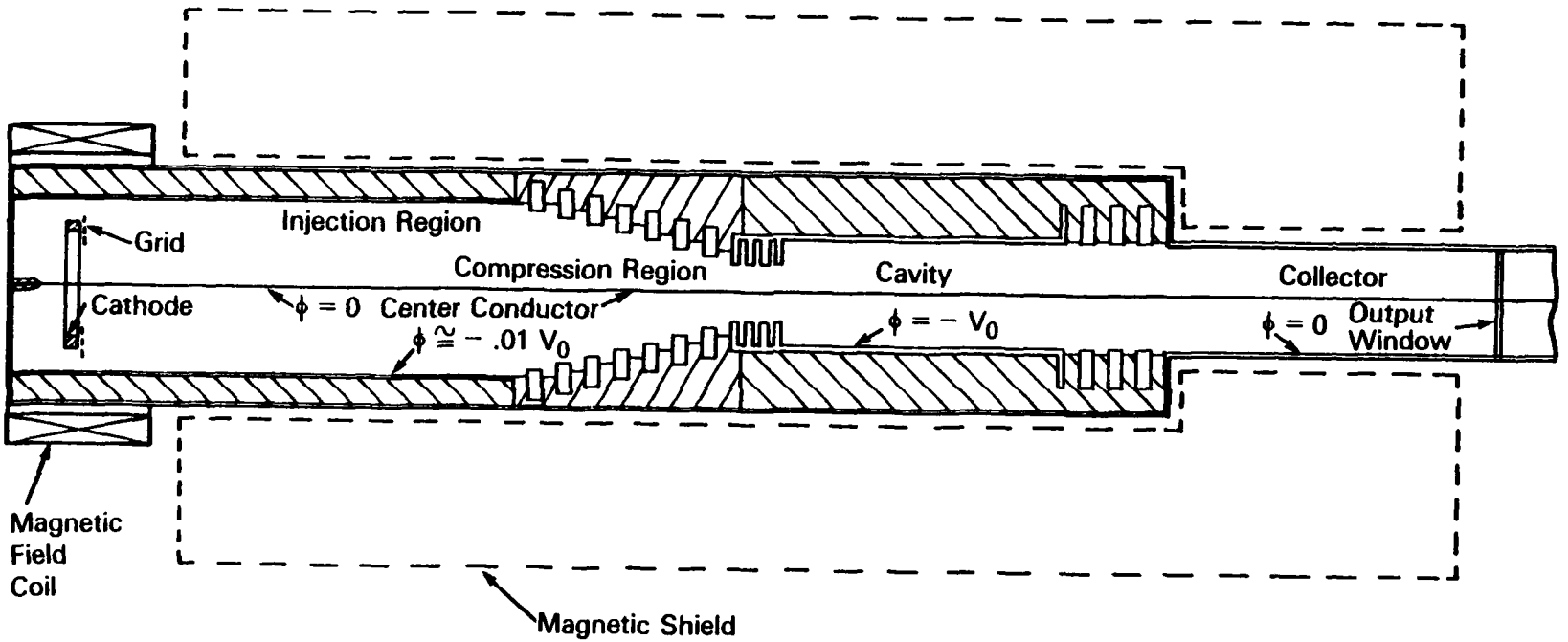

Figure 20. A conceptual design of the axial injection TEM orbitron.

IX. REFERENCES

Alexeff, I., and Dyer, F. (1980 a). *Phys. Rev. Lett.* **45**, 351-354.

Alexeff, I., and Dyer, F. (1980 b). *Laser Focus* **16**, 28-32.

Alexeff, I., and Dyer, F. (1983). *Proc. Int. Conf. on Infrared and Millimeter Waves (IEEE, New York)*, **F2.4**.

Alexeff, I., and Dyer, F. (1984). *Proc. 1984 Int. Conf. on Plasma Physics* (M.Q. Tran et al., eds.), p. 394, Ecole Polytechnique Federal de Lausanne, Lausanne, Switzerland.

Alexeff, I., (1985). Phys. Fluids **28**, 1990-1994.

Briggs, R.J. (1964). "Electron Stream Interaction with Plasma" Chapter 2, MIT Press, Cambridge, Massachusetts.

Chu, K.R. (1978). *Phys. Fluids* **21**, 2354-2364.

Hirshfield, J.L. (1979). Gyrotrons, In "Infrared and Millimeter Waves" (K. Button, ed.), Vol. 1, pp. 1-54. Academic Press, New York.

Hooverman, R.H. (1963). *J. of Appl. Phys.* **34**, 3505-3508.

Lau, Y.Y., Chu, K.R., Barnett, L.R. and Granatstein, V.L. (1981). *Int. J. Infrared Millimeter Waves* **2**, 373-393.

Lau, Y.Y., and Chernin, D. (1984 a). *Phys. Rev. Lett.* **52**, 1425-1428.

Lau, Y.Y., and Chernin, D. (1984 b). *Phys. Fluids* **27**, 2319-2331.

Ott, E., and Manheimer, W.M. (1975). IEEE Trans. Plasma Sci. **PS-3**, 1-5.

Schumacher, R.W., and Harvey, R.J., (1984). *Bull. Am. Phys. Soc.* **29**, 1179.

END

FILMED

3 -86

DTIC